THE JOURNAL OF COMPARATIVE NEUROLOGY 502:1–18 (2007)

Localization of the Transcriptional Coactivator PGC-1α to GABAergic Neurons during Maturation of the Rat Brain

RITA MARIE COWELL,[1,2] KATHRYN ROSE BLAKE,[2] AND JAMES W. RUSSELL[3,2,4]*
[1]Department of Psychiatry, University of Alabama, Birmingham, Alabama 35294
[2]Department of Neurology, University of Michigan, Ann Arbor, Michigan 48109
[3]Veterans Affairs Medical Center, Baltimore, Maryland 21201
[4]Department of Neurology, University of Maryland, Baltimore, Maryland 21201

ABSTRACT

The transcriptional coactivator peroxisome proliferator activated receptor γ coactivator 1α (PGC-1α) can activate a number of transcription factors to regulate mitochondrial biogenesis and cell-specific responses to cold, fasting, and exercise. Recent studies indicate that PGC-1α knockout mice exhibit behavioral abnormalities and progressive vacuolization in various brain regions. To investigate the roles for PGC-1α in the nervous system, we evaluated the temporal and cell-specific expression of PGC-1α in the normal developing rat brain. Western blot of whole brain homogenates with a PGC-1α-specific antibody revealed that PGC-1α protein was most abundant in the embryonic and early postnatal forebrain and cerebellum. Using quantitative reverse-transcriptase polymerase chain reaction (RT-PCR), we determined that PGC-1α mRNA expression increased most markedly between postnatal days 3 (P3) and 14 in the cortex, striatum, and hippocampus. Immunohistochemical and immunofluorescence analyses of brain tissue indicated that while PGC-1α was found in most neuronal populations from embryonic day 15 to P3, it was specifically concentrated in GABAergic populations from P3 to adulthood. Interestingly, PGC-1α colocalized with the developmentally regulated chemoattractant reelin in the cortex and hippocampus, and the survival-promoting transcription factor myocyte enhancing factor 2 was highly concentrated in GABAergic populations in the striatum and cerebellum at times of PGC-1α expression. These results implicate PGC-1α as a regulator of metabolism and/or survival in GABAergic neurons during a phase of mitochondrial and synaptic changes in the developing brain and suggest that PGC-1α may be a good target for increasing metabolism in GABAergic populations in neurodevelopmental and neurodegenerative disorders. J. Comp. Neurol. 502:1–18, 2007.

Indexing terms: metabolism; glutamic acid decarboxylase 67; reelin; myocyte enhancing factor 2

With the discovery that mutations in transcriptional repressors or coactivators can be causative for neurodevelopmental disorders such as Rett's syndrome and Rubinstein-Taybi syndrome (MeCP2 and CREB-binding protein, respectively; Petrij et al., 1995; Amir et al., 1999; Hong et al., 2005), research on the transcriptional control of postnatal brain development has come to the forefront. In this article we present another potential player in the transcriptional control of development: peroxisome proliferator activated receptor γ (PPARγ) coactivator 1α (PGC-1α). Initially described as a transcriptional coactivator of PPARγ and mediator of adaptive thermogenesis in adipose tissue (Puigserver et al., 1998), PGC-1α has since been implicated in a variety of cellular processes, including the metabolic responses to fasting (Lehman et al., 2000) and exercise (Knutti and Kralli, 2001; Baar et al., 2002).

Central to PGC-1α's role in cellular physiology is its ability to activate the transcription of genes involved in mitochondrial respiration and biogenesis (Scarpulla, 2002). PGC-1α is a transcriptional *co*activator, meaning

Grant sponsor: National Institute of Neurological Disorders and Stroke (NINDS); Grant number: NRSA awards T32 NS07222 and F32 NS049863 (to R.M.C.); Grant sponsor: National Institutes of Health (NIH); Grant number: NS42056; Grant sponsor: Office of Research Development (Medical Research Service); Grant sponsor: Department of Veterans Affairs; Grant sponsor: Juvenile Diabetes Research Foundation Center for the Study of Complications in Diabetes; (to J.W.R.) Grant sponsor: National Institute of Diabetes and Digestive and Kidney Diseases (NIDDK); Grant number: NIH 5P60DK-20572 (MDRTC).

*Correspondence to: James W. Russell, Department of Neurology, 22 South Greene Street, Baltimore, Maryland 21201.
E-mail: JRussell@som.umaryland.edu

Received 30 January 2006; Revised 1 June 2006; Accepted 19 September 2006

DOI 10.1002/cne.21211

Published online in Wiley InterScience (www.interscience.wiley.com).

TABLE 1. List of Antibodies

Target	Host	Antigen	Dilution	Specificity proven by	Source/cat. #/lot #
PGC-1α	Rabbit	a.a. 1-120 of mouse PGC-1α	1:20,000 (WB) 1:7500 (IHC) 1: 5000 (IF)	Western blot (91 kD), overexpression, nuclear localization	Custom from Quality Controlled Biochemicals, Hopkinton, MA; Animal #91378 Bleed #8
Actin	Mouse	a.a. 50-70 of chicken actin (conserved)	1:40,000 (WB)	Western blot (42 kD)	Chemicon, Temecula, CA; MAB1501R 0507003686
NeuN	Mouse Clone A60	Neuronal Nuclei Protein from mouse	1:1000 (WB, IHC, IF)	Western blot (46 kD), nuclear localization	Chemicon MAB377 25010730
TuJ1 (β-tubulin)	Mouse	Microtubules from rat brain	1:5000 (WB) 1:2000 (IHC, IF)	Western blot (50 kD), presence in cortical plate	Covance Research Products, Denver, PA; MMS-435P 147907002
Microtubule associated protein 2A and 2B	Mouse	Purified rat MAP2	1:200 (WB, IHC, IF)	Western blot (280 and 300 kD), presence in cortical plate	Chemicon AB5622
Glutamic acid decarboxylase, isoform 67 (GAD67)	Mouse clone 1G10.2	a.a. 4-101 of human GAD67	1:4000 (WB) 1:2500 (IHC, IF)	Western blot (67 kD), in cytoplasm of cells with morphology and neuroanatomical location of inhibitory interneurons	Chemicon MAB5406 25030191
Reelin	Mouse	a.a. 164-496 of mouse reelin	1:500 (WB) 1:250 (IF)	Western blot (180, 300, and 400 kD), cytoplasmic localization, concentration in layer I of developing cortex	Chemicon MAB5364 0601020627
MEF2a	Rabbit	a.a. 487-507 of human MEF2a	1:500 (WB) 1:250 (IF) 2 μg/100 μg homogenate	Immunoprecipitation and Western blot (64-70 kD; Allen et al., 2000), nuclear localization, concentration in cerebellum as previously reported	Santa Cruz Biotechnology, Santa Cruz, CA; Sc-313 D1405

a.a., amino acid; WB: Western blot; IHC: immunohistochemistry; IF: immunofluorescence; IP: immunoprecipitation.

that it facilitates the interactions of transcription factors and their activating proteins to form functional DNA-binding complexes. PGC-1α cannot bind DNA or activate transcription alone, so its downstream effects are completely dependent on coexpressed transcription factors. To regulate metabolic genes, PGC-1α interacts with nuclear respiratory factor 1 (NRF-1) and the nuclear respiratory factor 2 complex, composed of GA-binding protein α and β subunits (GABPα, β). Transient overexpression of PGC-1α in nonneuronal cells increases the expression of cytochrome c oxidase subunits (Scarpulla, 2002), ATP synthase β (Villena et al., 1998), and mitochondrial transcription factor A, as well as uncoupling proteins (Tiraby et al., 2003) and antioxidant enzymes (St-Pierre et al., 2003).

Several recent reports suggest that PGC-1α has critical roles in neuronal function and signaling. Mice lacking the gene for PGC-1α demonstrate progressive vacuolization in various brain regions within the first 3 months of age and exhibit abnormal behavioral characteristics (Lin et al., 2004; Leone et al., 2005). In addition, PGC-1α expression can be regulated by neuronal activity in vitro and in vivo (Liang and Wong-Riley, 2006). From studies in nonneuronal cells, it is clear that PGC-1α has the potential to interact with a variety of transcription factors that influence neuronal signaling, plasticity, and survival. PGC-1α can coactivate estrogen and estrogen-related receptors (Bramlett and Burris, 2002; Kressler et al., 2002; Schreiber et al., 2004), the thyroid hormone receptor (Zhang et al., 2004), glucocorticoid receptors (Herzig et al., 2001; Yoon et al., 2001), and members of the myocyte enhancing factor 2 (MEF2) family (Czubryt et al., 2003). Of note, its expression can be regulated by calcium/calmodulin-dependent protein kinase II (CaMKII) and IV and cAMP-responsive element binding protein (CREB; Herzig et al., 2001; Yoon et al., 2001), and PGC-1α may play a role in the physiological signaling of nitric oxide (Nisoli et al., 2003).

To determine the possible causes for the observed phenotype in the knockout mice and the roles for PGC-1α in brain development and function, we evaluated its temporal and cell-specific expression throughout forebrain and cerebellar development in the rat. In addition, to identify potential functions for PGC-1α in vivo, we investigated whether PGC-1α was coexpressed with the chemoattractant reelin and the transcription factor myocyte enhancing factor 2 (MEF2), which interacts with PGC-1α in nonneuronal cells.

ABBREVIATIONS

EGL	External granule cell layer
IGL	Internal granule cell layer
GABA	γ-Aminobutyric acid
GAD67	Glutamic acid decarboxylase 67 (GAD1)
MEF2	Myocyte enhancing factor 2
ML	Molecular cell layer
PGC-1α	Peroxisome proliferator activated receptor γ coactivator 1α
PL	Purkinje cell layer

MATERIALS AND METHODS

Antibodies

For a comprehensive list of the antibodies and their characteristics, see Table 1. Briefly, antibodies included rabbit anti-PGC-1α (gift of Daniel P. Kelly, Center for Cardiovascular Research, Washington University; Lehman et al., 2000), rabbit anti-MEF2, mouse anti-β-tubulin III, mouse microtubule associated protein 2 (MAP2), mouse anti-actin, mouse anti-NeuN, mouse anti-rodent reelin, and mouse anti-glutamic acid decarboxylase (67 kD isoform). The specificities of all antibodies were tested by Western blotting (see procedure below). Staining patterns from immunohistochemistry experiments were found to be identical to those seen with immunofluorescence, and the neuroanatomical and subcellular localization of immunoreactivity for all antibodies (except PGC-1α) was similar to what has been previously reported.

Tissue preparation

Animals were sacrificed at embryonic days (E)15, E18, E21, postnatal days (P)3, P7, P14, P21, or 3 months of age (adult). For embryonic timepoints, dams were euthanized with sodium pentobarbital (100 mg/kg), pups were removed, and brains were either frozen immediately for RNA extraction, added to homogenization buffer for Western blotting, or drop-fixed in 4% paraformaldehyde for immunohistochemistry (see below). For isolation of postnatal tissue for reverse-transcriptase polymerase chain reaction (RT-PCR) and Western blotting, animals were euthanized with sodium pentobarbital. For immunohistochemistry, postnatal animals were anesthetized with a mixture of ketamine (60 mg/kg) and xylazine (5 mg/kg) and perfused intracardially with phosphate-buffered saline (PBS, pH 7.4) and 4% paraformaldehyde in PBS. All animal protocols were approved by the University of Michigan and VA Medical Center centers for use of laboratory animals.

Semiquantitative Western blot analysis

For animals ages E15–E21, whole brains were homogenized in RIPA buffer (150 mM NaCl, 1% Triton X-100, 0.5% sodium deoxycholate, 0.1% lauryl sulfate in 50 mM Tris, pH 8.0) with 2% CHAPS (for the solubilization of mitochondrial proteins) and protease inhibitors (Roche Diagnostics, Indianapolis, IN). For ages P3–P21, single hemispheres were used. For animals older than 21 days a coronal block of tissue from one hemisphere (from approximately bregma 1.0 through bregma −6.0) was isolated for homogenization. Tissues were homogenized 30 strokes at maximum speed with a Tissue Tearor (Research Products International, Mount Prospect, IL) and centrifuged at 13,000 rpm for 30 minutes. The supernatant was frozen at −80°C until use or immediately mixed in sample buffer (20% glycerol, 2% lauryl sulfate, 0.2 M dithiothreitol, and 0.3 mM bromophenol blue in 167 mM Tris, pH 6.8) and boiled 5 minutes. Protein content was determined using bovine serum albumin as a standard (Pierce Biotechnology, Rockford, IL). To confirm that the centrifugation process did not influence the isolation of PGC-1α, another set of forebrain samples (E21–P28; n = 3/age group) was collected, homogenized (100 mg/mL homogenization buffer), and then boiled immediately in sodium dodecyl sulfate (SDS) sample buffer without centrifugation. Proteins were separated with SDS polyacrylamide gel electrophoresis (PAGE) electrophoresis on 8% polyacrylamide gels (10 μg/lane; Invitrogen, Carlsbad, CA) and transferred to nitrocellulose membranes (Bio-Rad Laboratories, Hercules, CA), and Western blotting was performed as described by Cell Signaling Technology (Danvers, MA), with slight modifications. Briefly, blocking was performed for 1 hour with 5% dry milk in Tris-buffered saline (TBS; 0.15 M NaCl, 0.02 M Tris, pH 7.6), and the membrane was incubated with the primary antibody in 5% IgG-free BSA (Jackson Immunoresearch, West Grove, PA) overnight at 4°C and then with the peroxidase-conjugated secondary antibody (Jackson Immunoresearch) in 5% milk for 1 hour. Signal was detected with enhanced chemiluminescence (Amersham Biosciences, Piscataway, NJ) and exposure to Biomax Kodak film (Eastman Kodak, Rochester, NY). Films were scanned and imported into ImageQuant 5.2 software for the estimation of band intensity. Three developmental time courses (E15 to adult; eight animals per set) were run on separate gels, and all values were normalized to actin and then compared to the P3 value on the same gel. Values are expressed as percent of the P3 value ± standard error.

To generate a positive control for the PGC-1α Western, we transfected SH-SY5Y neuroblastoma cells (MOI: 25:1) with an adenovirus for mouse PGC-1α (generously provided by Bruce M. Spiegelman, Dana Farber Research Institute and Harvard University; Lin et al., 2003) for 48 hours, collected the cells in RIPA buffer as above, and processed the samples for PGC-1α Western blotting.

Quantitative RT-PCR

E18 to adult brains were removed and placed on ice for the isolation of the hippocampus, cortex, striatum, thalamus, and cerebellum. Tissue pieces were collected in centrifuge tubes and snap-frozen in liquid nitrogen. RNA was isolated by the Trizol method following manufacturer's instructions (Invitrogen), with chloroform and isopropanol, was washed in ethanol, and resuspended in RNAse-free water. Equivalent amounts of RNA (2.5 μg) were treated with DNase I at 37°C for 30 minutes (1 unit DNase per μg RNA; Promega, Madison, WI), DNase was inactivated at 65°C for 15 minutes, and RNA was reverse-transcribed using the High-Capacity cDNA Archive Kit (Applied Biosystems, Foster City, CA). Taqman PCR was performed with mastermix (Applied Biosystems) and primers for eukaryotic 18s rRNA or PGC-1α mRNA (Applied Biosystems; Cat. Nos. Hs99999901_s1 and Rn00580241_m1, respectively). 18s has been used previously as a standard in brain development (Al-Bader and Al-Sarraf, 2005), as 18s content is directly correlated with total RNA content (Schmittgen and Zakrajsek, 2000). Reactions were run performed with an initial ramp time of 2 minutes at 50°C and 10 minutes at 95°C, and 40 subsequent cycles of 15 seconds at 95°C and 1 minute at 60°C. As a negative control for the RT reaction, reverse transcriptase was omitted in the reaction mix. For negative controls for the PCR reaction, either the primer sets or the cDNA were omitted from the reactions. Relative concentrations of PGC-1α or 18s RNA were calculated with comparison to a standard curve made with dilutions of cDNA from E21 thalamus. Values for PGC-1α were normalized to 18s values for the same samples; values are expressed as arbitrary units (ratio of PGC-1α to 18s) ± standard error.

Immunohistochemistry

Brains were removed, postfixed in paraformaldehyde for 24–72 hours at 4°C, cryoprotected in graded sucrose solutions (5–20%), embedded 1:1 in 20% sucrose and OCT media (VWR, West Chester, PA), and frozen at −80°C. Tissue blocks were sectioned at 20 μm, mounted on charged slides (Fisher, Hampton, NH), and allowed to dry overnight before freezing at −80°C until use. For immunohistochemistry and immunofluorescence, slides were thawed, rinsed 5 minutes, and blocked with 10% serum from the host of the secondary antibody in PBS, pH 7.4. If no antigen retrieval process was required (see below), sections were incubated with the primary antibody overnight in PBS with 0.3% Triton X-100 at 4°C. All optimal dilutions for primary antibodies were determined with and without the antigen retrieval step. After incubation with the primary antibody, sections were washed, incubated 1 hour with the corresponding secondary antibody,

peroxidase-quenched with 0.3% hydrogen peroxide in methanol, and incubated with the horseradish-peroxidase-labeled ABC reagent (Vector Laboratories, Burlingame, CA) for 30 minutes. After washing, antibody binding was visualized with diaminobenzamide. Stained sections were dehydrated in graded ethanols and xylenes and mounted with nonaqueous mounting media. Selected images were captured using a SPOT camera attached to a Nikon Microphot-SA light microscope with 4×, 10×, 20×, and 60× objectives, and images were imported into Adobe Photoshop 7.0 (San Jose, CA) for processing. Images were adjusted for brightness, contrast, and sharpness.

To rule out nonspecific binding of the secondary antibody and autofluorescence, primary antibodies were replaced with species-matched nonspecific IgG.

Immunofluorescence and confocal microscopy

For double- or triple-labeling immunofluorescence, sections were blocked with donkey serum and primary antibodies from different species were pooled and applied to sections overnight, as described above. Secondary antibodies, all made in donkey, were pooled and applied to sections for 1 hour at room temperature. Immediately after removal of the secondary antibodies, sections were incubated with DAPI (150 ng/mL; Molecular Probes, Eugene, OR) for 10 minutes for visualization of cell nuclei. After washing, sections were coverslipped with antifade media (Molecular Probes) and allowed to dry at room temperature overnight before storage at 4°C. Immunofluorescence was visualized in triple channel mode on an Olympus IX-71 inverted microscope (using a 20× air or 40× oil objective) equipped with an Olympus FluoView 500 confocal laser scanning imaging system at the Michigan Diabetes Research and Training Center (University of Michigan, Ann Arbor, MI). Data were collected from each channel sequentially and barrier filters minimized channel leak-through (430–460 nm barrier filter in the DAPI range and 505–525 nm barrier filter in the FITC range). The images from two or three channels were merged and the brightness and contrast of the images were adjusted with Adobe Photoshop 7.0.

Antigen retrieval

For antigen retrieval (required for optimal staining of β-tubulin, MAP2, PGC-1α, and GAD67), sections were blocked with 10% serum in PBS, incubated in citrate buffer (10 mM citric acid, pH 5.0) for 30 minutes at 37°C, rinsed for 5 minutes in PBS, then incubated with the primary antibody(ies) overnight, as above.

Statistical analysis

Western blotting and quantitative RT-PCR data were expressed as mean ± standard error. Significant differences among groups were determined using one-way analysis of variance (ANOVA). Post-hoc analyses to determine significant differences between individual groups were performed using a 2-tailed *t*-test, assuming unequal variances. Statistical significance was set at $P = 0.05$.

RESULTS

Detection of PGC-1α by Western blot

In initial experiments, we used a PGC-1α-specific antibody to detect PGC-1α in whole brain homogenates by Western blotting (Fig. 1A). As expected, the antibody detected a band of 91 kD; the signal was stronger in P3 brain than in adult brain. The antibody also recognized overexpressed PGC-1α (FLAG-tagged; Lin et al., 2003) in the neuroblastoma cell line SH-SY5Y at ~110 kD, indicating that the antibody specificity was sufficient for Western blot analysis.

To investigate changes in PGC-1α protein expression throughout brain development, we performed Western blots for PGC-1α on whole forebrain and whole cerebellum homogenates from embryonic (E15, E18, E21) and postnatal (P3, P7, P14, P21, P90) animals (n = 3/age group). Three sets of developmental time courses were run on separate gels and band intensity was estimated with normalization to actin (run on the same gel). PGC-1α signal declined progressively with age in the forebrain (Fig. 1B,C) in comparison to actin-β. Signal for PGC-1α was strong in animals age E15 to P14, low at P21, and undetectable in adult brain homogenates. In the postnatal cerebellum, PGC-1α signal was strong from P3–P21 and reduced, but still detectable, in the adult. While others have reported that actin expression at the RNA level changes in development, we did not see any influence of age on actin protein expression. Values are expressed as percent of the P3 value from the same gel. Results from each sample set were consistent and demonstrated a decrease in PGC-1α with developmental age in the forebrain ($P < 0.01$, one-way ANOVA) and a significant decrease by adulthood in the cerebellum ($P < 0.01$, one-way ANOVA). To investigate the possibility that a significant amount of PGC-1α was trapped in the pellet after centrifugation, we processed a separate set of samples without centrifugation and boiled the samples directly in SDS sample buffer. While the signal for PGC-1α was slightly increased in the older (P28) tissue samples, the overall trend was the same. Intensity values (percent of one P3 value ± SE) for each age were as follows: E21, 201 ± 57; P3, 133 ± 23; P7, 102 ± 42; P14, 43 ± 23; P21, 50 ± 19; P28, 28 ± 19. PGC-1α expression differed among age groups (n = 3/age group; $P < 0.01$; one-way ANOVA) and decreased significantly between P3 and P14 ($P < 0.03$; *t*-test).

Regional analysis of PGC-1α mRNA expression by quantitative RT-PCR

While the Western blot results indicated that PGC-1α protein was more abundant during prenatal brain development than postnatal development, these data were limited by the fact that Western blot is often insensitive (PGC-1α could be expressed in adult animals even though there was little signal) and that Western results from whole brain homogenates give no indication of neuroanatomical distribution. To evaluate region-specific changes in PGC-1α expression, we isolated four brain regions reported to be most affected in the knockout animals (striatum, hippocampus, cortex, and thalamus) and one area that was only mildly affected (cerebellum) from animals of different ages, using 18s rRNA as an internal standard (see Materials and Methods). 18s RNA signal (arbitrary units ± SE) remained constant with age in all regions (i.e., thalamus: E21, 0.85 ± 0.08; P3, 0.89 ± 0.07; P7, 0.86 ± 0.04; P14, 0.89 ± 0.07; P21, 0.85 ± 0.04; adult, 0.84 ± 0.08; n = 4–5/age group; $P = 0.99$, one-way ANOVA).

PGC-1α mRNA expression profiles differed markedly from region to region, and substantial mRNA expression was detected in adult brain in all regions tested (Fig. 2). Of the five

regions evaluated, thalamus was the only region that showed no measurable change in PGC-1α mRNA expression with age (n = 3–6/age group; $P = 0.36$; one-way ANOVA). In the other four regions (striatum, cortex, hippocampus, and cerebellum), mRNA expression changed significantly with developmental age (n = 3–6/age group; $P < 0.01$ for all; one-way ANOVA). Post-hoc statistical analysis (*t*-test, two-sample assuming unequal variances) revealed that PGC-1α expression in the P7 striatum was significantly greater than in the P3 striatum ($P = 0.02$) and that RNA expression decreased in the adult with respect to P14 animals ($P = 0.05$). In the cortex, a marked increase in RNA expression was observed between P7 and P14 ($P < 0.01$), but there was not a significant difference between P14 and adult values ($P = 0.1$). PGC-1α expression in the hippocampus looked similar to that in the striatum, with an increase detected between P7 and P14 ($P = 0.03$), and expression was decreased significantly in the adult in comparison to P14 hippocampus ($P = 0.04$). In contrast, in the cerebellum, expression at P14 was significantly lower than expression at P3 ($P = 0.02$).

Comparison among regions of P3, P14, and adult brain (Fig. 2F) indicated that PGC-1α expression varied by region (P3: $P < 0.01$; P14, adult: $P \leq 0.01$; one-way ANOVA). Of note, the cortex expressed the least amount of PGC-1α at P3 ($P < 0.01$; *t*-test) and the cerebellum expressed more PGC-1α than the striatum ($P = 0.04$) or hippocampus ($P = 0.05$) in adults.

Regional analysis of PGC-1α expression with immunohistochemistry and light microscopy

One report has indicated that PGC-1α RNA is expressed throughout the mouse brain (Tritos et al., 2003), but its cellular localization in development and adulthood in the rat is unknown. To determine the regional and cell-specific expression of PGC-1α during brain development, we used immunohistochemistry and immunofluorescence with the antibody proven to be specific for PGC-1α by Western blot (Fig. 1). Initial immunohistochemical assays showed very little specific staining; because the antibody worked well for Western blotting, we hypothesized that an antigen retrieval step was required (citrate buffer preincubation, see Materials and Methods). With this procedure, widespread PGC-1α immunoreactivity was observed throughout the brain at all ages tested. To allow comparison of intensity across ages, sections from each developmental age were included in all experiments. At low magnification, it was clear that the intensity of staining in gray matter correlated well with the Western blotting results; with increasing age, the overall intensity of staining decreased. However, at higher magnification, it was evident that staining in embryonic brain was not concentrated highly within cell bodies, but diffuse throughout the forming cortical plate and in gray matter areas. Inter-

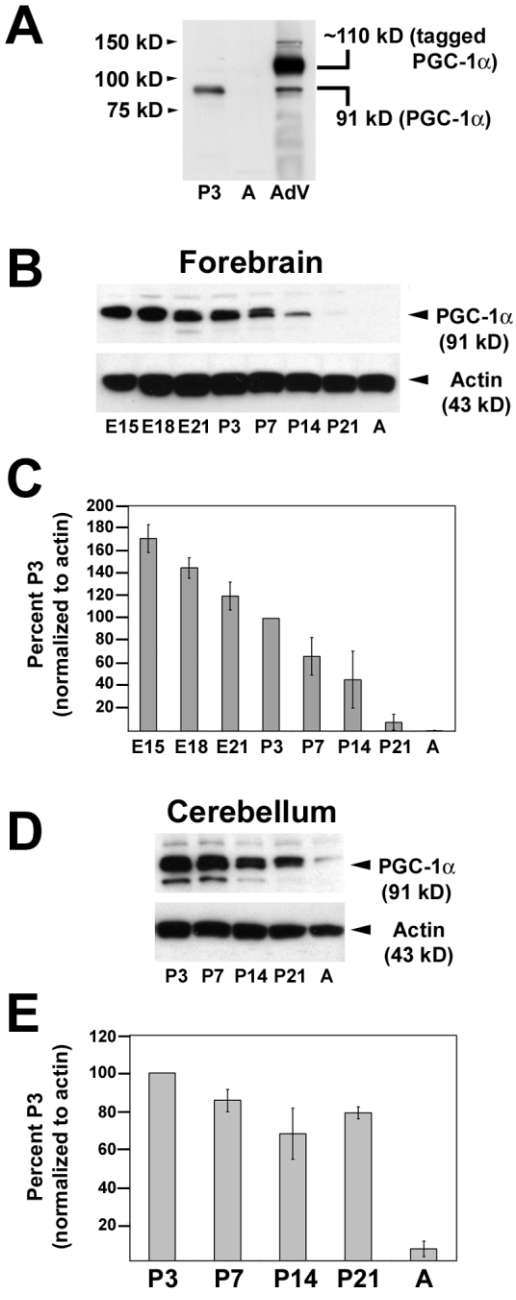

Fig. 1. The abundance of PGC-1α protein decreases during forebrain and cerebellar development. Using an antibody specific for PGC-1α, PGC-1α protein was detected in whole forebrain and cerebellum homogenates from embryonic and postnatal rats. **A:** Native PGC-1α (91 kD) is detectable in P3 forebrain. The antibody recognizes both native and FLAG-tagged PGC-1α (~110 kD), overexpressed with an adenovirus in the SH-SY5Y neuroblastoma cell line (AdV). In this film no PGC-1α was detectable in the adult (A) forebrain sample. **B:** PGC-1α protein is detectable from E15 through P14 forebrain but not in P21 or adult samples; the intensity of the band decreases with developmental age. **C:** Relative intensity of the PGC-1α band was measured (see Materials and Methods), with reference to the P3 sample on the same gel, and normalized to the intensity of the actin band. The intensity of the PGC-1α band decreases significantly with age ($P < 0.01$, n = 3/age group). **D:** PGC-1α protein was detected in cerebellar homogenates from postnatal rat brain; similar to the results seen for forebrain samples, the intensity of the band was more pronounced in younger animals. **E:** The intensity of the PGC-1α and actin bands were quantified, and values are expressed as a percent of the intensity of the P3 sample on the same gel. The signal intensity of adult samples was significantly decreased with respect to samples from younger animals ($P < 0.01$; n = 3/age group).

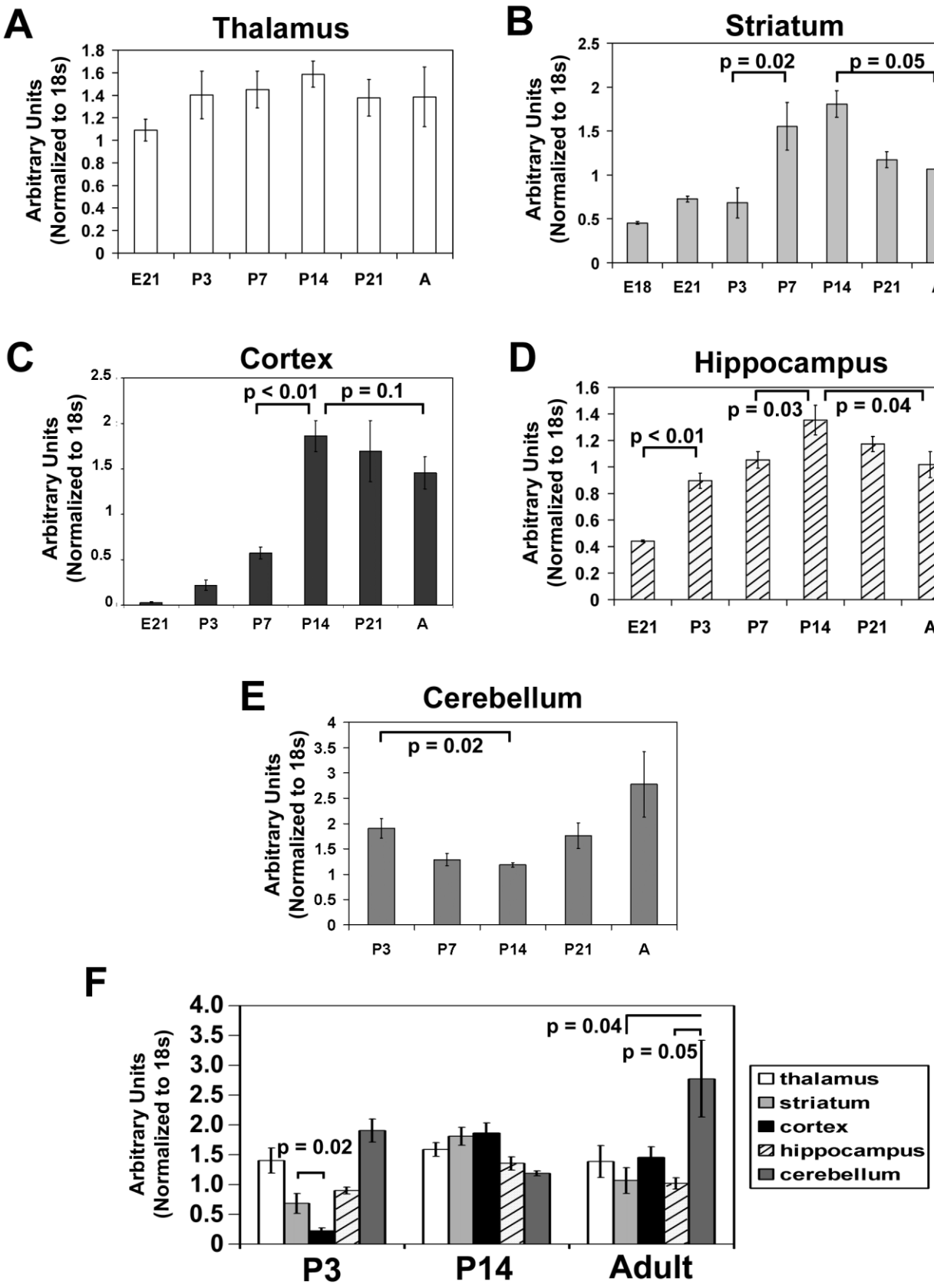
A
Thalamus
Arbitrary Units (Normalized to 18s)
E21
P3
P7
P14
P21
A
B
Striatum
p = 0.02
p = 0.05
E18
C
Cortex
p < 0.01
p = 0.1
D
Hippocampus
p < 0.01
p = 0.03
p = 0.04
E
Cerebellum
p = 0.02
F
p = 0.04
p = 0.05
p = 0.02
P3
P14
Adult
thalamus
striatum
cortex
hippocampus
cerebellum

Figure 2

estingly, at later ages (P7 to adulthood), immunoreactivity was found specifically in cell bodies, and less in processes.

Cortex. In coronal sections of E15 brain, PGC-1α immunoreactivity was widespread, but most concentrated in the forming cortical plate (CP, Fig. 3A,E). To determine the correlation between the appearance of PGC-1α immunoreactivity and the appearance of neurons in the embryonic brain, we compared PGC-1α immunoreactivity to NeuN, MAP2, and β-tubulin immunoreactivity (Fig. 3A–F). The pattern of PGC-1α immunoreactivity corresponded most closely with immunoreactivity for NeuN and MAP2; only faint staining for PGC-1α was detectable in the β-tubulin-positive intermediate zone.

PGC-1α was also localized to the cortical plate at E18 (Fig. 3G–J) and E21 (not shown). While PGC-1α immunoreactivity was faint in the cortical subplate (SP; Fig. 3G,I), it was concentrated in regions of NeuN immunoreactivity (Fig. 3H,J). PGC-1α immunoreactivity was present at the same location and developmental stages as NeuN immunoreactivity in all regions evaluated.

In early postnatal cortex (P3), PGC-1α immunoreactivity (Fig. 3K) was widespread in areas of NeuN immunoreactivity (Fig. 3L). However, in contrast to E18 and E21 cortex, distinct PGC-1α staining was found in individual cell bodies (Fig. 3K, arrowheads). At P7 (not shown) and P14 (Fig. 3M,N), more darkly stained cell bodies were observed (Fig. 3M, arrowheads) as the density of NeuN-stained cells decreased (Fig. 3N). In adulthood (P90), all PGC-1α-specific staining was localized to cell bodies (Fig. 3O). Of note, there were fewer PGC-1α-positive cells than NeuN-positive cells (Fig. 3P) in the adult cortex. With respect to laminar organization, the greatest number of PGC-1α-positive cells were noted in Layers II and III of the cortex, where the staining for glutamic acid decarboxylase 67 (GAD67) was the most intense (Fig. 3Q). In Layers II/III (Fig. 3R) and IV (Fig. 3S), small cells were immunoreactive for PGC-1α (arrowhead), while larger cells displayed only faint staining (Fig. 3S, arrows). Little staining could be attributed to the secondary antibody alone (primary antibody replaced with nonspecific rabbit IgG; Fig. 3T).

Hippocampus. Staining for PGC-1α was present in areas of NeuN immunoreactivity in the embryonic hippocampus at E18 and E21 (not shown). In P3 and all older animals, faint cellular immunoreactivity for PGC-1α was noted in all regions with NeuN immunoreactivity, with concentrated staining in few cells. Representative images are shown from the adult hippocampus (Fig. 4). At low magnification, PGC-1α immunoreactivity was visible throughout the pyramidal cell layer (CA1, CA3 regions), subiculum, and dentate gyrus (Fig. 4A), with few scattered immunoreactive cells outside these neuronal layers. At higher magnification, faint PGC-1α immunoreactivity was noted in cells of the dentate gyrus (Fig. 4B,D) in a pattern similar to NeuN (Fig. 4C,E), with few being intensely immunoreactive for PGC-1α (Fig. 4B, arrowhead; Fig. 4D). Just adjacent to the dentate gyrus, large PGC-1α-positive cells were noted (Fig. 4F,H) with a staining pattern similar to NeuN (Fig. 4G,I). This was the case for other regions of the hippocampus as well, including the CA3 region of the pyramidal cell layer.

Striatum. Due to the possible role of PGC-1α in striatal function (Lin et al., 2004), we also investigated the distribution of PGC-1α immunoreactivity in the striatum (Fig. 4J–M). Most cells demonstrated little to no specific staining, while a small percentage of cells were intensely immunoreactive for PGC-1α (Fig. 4J,L). PGC-1α-positive cells were in the same location and had the morphology of NeuN-positive neurons (Fig. 4K,M).

Cerebellum. Immunohistochemistry for PGC-1α in sagittal sections of cerebellum indicated that PGC-1α was concentrated in multiple neuronal populations in the developing and adult cerebellum. At P3, when Purkinje cells were aligning to form the Purkinje cell layer (PL), they were intensely immunoreactive for PGC-1α (Fig. 5A,B). Little staining was seen in the external granule cell layer (EGL; Fig. 5B). Neurons of the cerebellar deep nuclei were also PGC-1α-positive (Fig. 5A,C). In the adult cerebellum (Fig. 5D–F), the granule cells had migrated into the internal granule cell layer (IGL), and the Purkinje cells had formed a monolayer (Fig. 5D). Purkinje cells (arrowheads, Fig. 5D,E), cells in the IGL, and scattered cells in the molecular cell layer (ML; arrows, Fig. 5D,E) were PGC-1α-immunoreactive, as were neurons in the deep cerebellar nuclei (Fig. 5F). The pattern of PGC-1α immunoreactivity in the ML and deep nuclei was similar to that observed for NeuN and β-tubulin (not shown).

PGC-1α and GABA. More thorough analysis of PGC-1α immunoreactivity patterns throughout the developing brain revealed an interesting pattern. PGC-1α was most concentrated in regions with neurons that produce the neurotransmitter γ-aminobutyric acid (GABA), and the cellular distribution of PGC-1α-positive cells in the cortex, hippocampus, and cerebellum mirrored the distribution of GABAergic neurons in those regions. As an example, images from one GABAergic region, the globus pallidus (GP), are presented (Fig. 5G–J). At P3, the neurons within the globus pallidus were densely populated and strongly immunoreactive for PGC-1α (Fig. 5G,H). In contrast, few cells within the neighboring striatum (Str) were PGC-1α-positive (Fig. 5G). Globus pallidus neurons in the adult brain were also strongly positive for PGC-1α

Fig. 2. Analysis of PGC-1α mRNA expression in the thalamus, striatum, cortex, hippocampus, and cerebellum. To determine if PGC-1α expression varied by region in the developing rat brain, five brain areas (thalamus, striatum, cortex, hippocampus, and cerebellum) were dissected and processed for quantitative RT-PCR for PGC-1α (n = 3-6/age group). The signal from each sample was normalized to the same sample's 18s rRNA content. To allow comparisons among all samples tested, the same standards were used for every PCR reaction. Values are expressed as arbitrary units ± standard error, after normalization to 18s rRNA content. *P* values for post-hoc *t*-tests are labeled on each graph. **A:** PGC-1α mRNA expression was detectable in thalamus at all ages tested; expression did not change with developmental age ($P = 0.36$). **B:** PGC-1α mRNA expression changed significantly with age in striatum ($P < 0.01$, one-way ANOVA), with a significant increase occurring between P3 and P7 and a decrease between P14 and adult. **C:** In the cortex, PGC-1α expression significantly differed among age groups ($P < 0.01$); expression increased significantly between P7 and P14, but did not decrease appreciably by adulthood. **D:** PGC-1α expression differed among samples ($P < 0.01$) in the hippocampus. Significant increases were detected between E21–P3 and P7–P14, and expression decreased between P14 and adult. **E:** In the cerebellum, PGC-1α mRNA was abundant at all ages and changed significantly with age ($P < 0.01$). **F:** To visualize region-specific changes in PGC-1α mRNA expression by age, the same data displayed in A–E is grouped by age. In early postnatal rat brain (P3), expression is lowest in the cortex. In P14 and adult samples, expression is widespread.

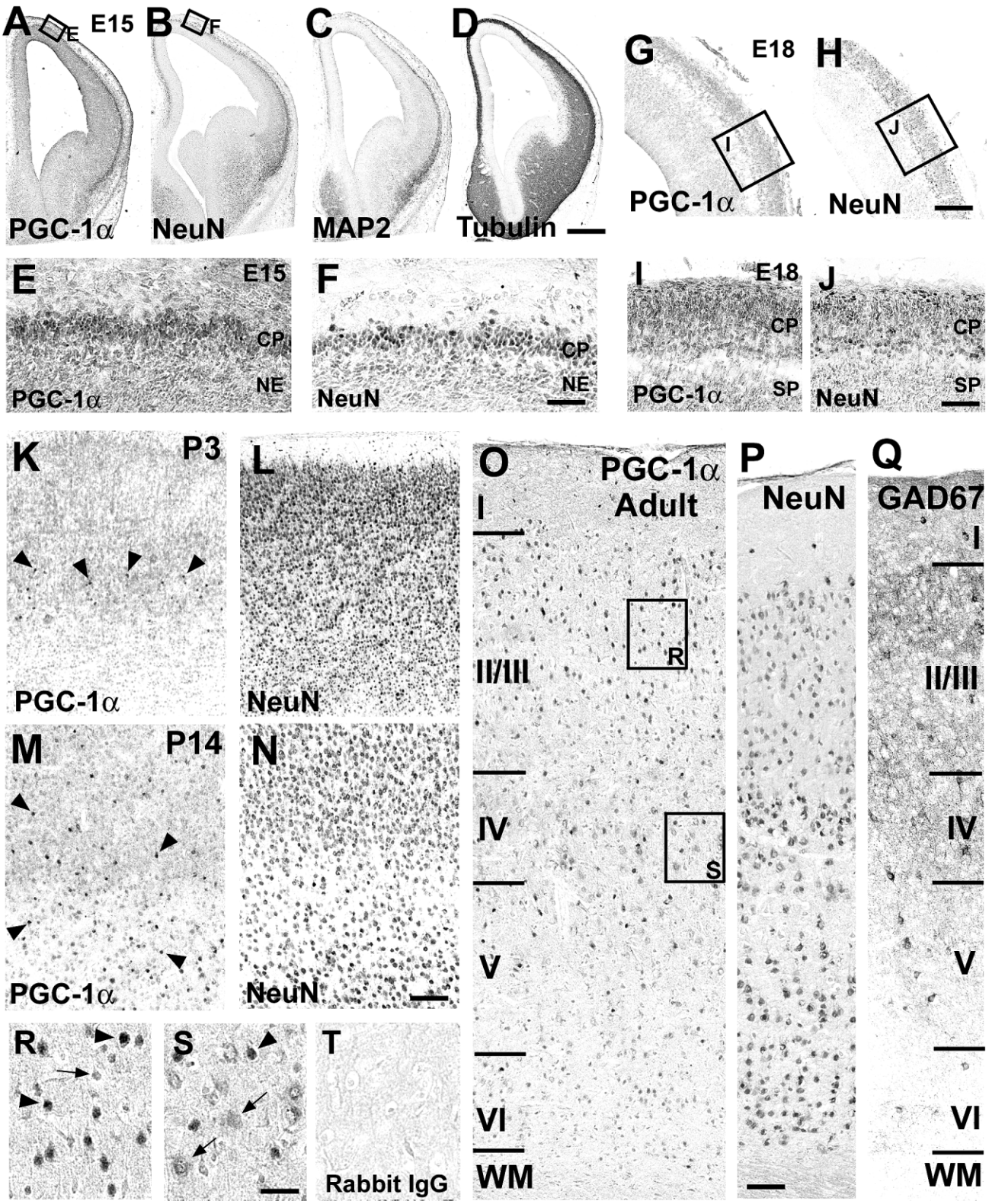
A
E
E15
B
F
C
D
PGC-1α
NeuN
MAP2
Tubulin
G
E18
H
I
J
PGC-1α
NeuN
E
E15
CP
NE
PGC-1α
F
CP
NE
NeuN
I
E18
CP
SP
PGC-1α
J
CP
SP
NeuN
K
P3
PGC-1α
L
NeuN
M
P14
PGC-1α
N
NeuN
O
PGC-1α
Adult
I
II/III
R
IV
S
V
VI
WM
P
NeuN
Q
GAD67
I
II/III
IV
V
VI
WM
R
S
T
Rabbit IgG

Figure 3

(Fig. 5I,J), although the density of PGC-1α-positive neurons was reduced at this age.

GABAergic thalamic nuclei such as the reticular nucleus of the thalamus also exhibited very intense PGC-1α immunoreactivity. Other regions that contained PGC-1α immunoreactive cell bodies, but that are not described in further detail here, include the olfactory bulb, hypothalamus, vestibular nucleus, brain stem reticular nuclei, red nucleus, nucleus of the solitary tract, trapezoid body and inferior olive, mammillary nucleus, habenula, piriform cortex, amygdala, and the lateral dorsal and ventrolateral nuclei of the thalamus. There was little staining in medial thalamic nuclei, mammillary bodies, or the deep pontine gray.

Cell-specific localization of PGC-1α with immunofluorescence and confocal microscopy

To localize PGC-1α to specific cell types in the developing brain, we used immunofluorescence and confocal microscopy. At P3 and earlier, PGC-1α immunoreactivity was not distinctively localized to cell bodies but was diffusely distributed throughout NeuN-positive areas (Fig. 3G–J,M,N). This diffuse pattern was confirmed with confocal microscopy (Fig. 6A). At P7, however, immunoreactivity was more concentrated in cell bodies (arrowheads, Fig. 6B) that were NeuN-positive (Fig. 6B2,B3). Faint staining was still observed in other cells, but was always associated with NeuN (arrows, Fig. 6B). At P14 a similar pattern was seen, with PGC-1α being concentrated in a low percentage of NeuN-positive cells. In most cases, PGC-1α-positive cells were small in comparison to neighboring cells (arrows, Fig. 6C). Notably, during this transition from diffuse homogeneous staining to cell-specific staining, cell size increased markedly (Fig. 6A,B, and C at same magnification). Also, thorough analysis of NeuN and PGC-1α colocalization indicated that PGC-1α immunoreactivity was rarely present in the absence of NeuN; PGC-1α immunoreactivity was consistently absent throughout development in white matter regions and areas of physiologically activated microglia (P7 and earlier). PGC-1α also colocalized with β-tubulin (see Fig. 6P) and MAP2 (not shown).

From the results with immunohistochemistry, we hypothesized that PGC-1α was present in GABAergic neurons. To test this idea, we investigated whether PGC-1α colocalized with the protein GAD67, one of two enzymes responsible for the conversion of glutamate to GABA (Kaufman et al., 1991). With the citrate buffer pretreatment, GAD67 immunoreactivity was detectable in the cytoplasm of cells as well as in cellular processes (green, Fig. 6D–H). Because many cells exhibited GAD67-positive synaptic contacts (arrows, Fig. 6E2), we classified GABAergic neurons by their cytoplasmic staining. Remarkably, most GAD67-positive neurons identified throughout the brain were immunoreactive for PGC-1α (red, Fig. 6D–H). In the P14 cortex, many PGC-1α-positive, GAD67-positive neurons were identified (arrowheads, Fig. 6D) in the vicinity of GAD67-negative cells with little PGC-1α immunoreactivity (arrows, Fig. 6D). In the adult cortex, GAD67-positivity was more intense; cytoplasmic staining was distinct in the cytoplasm of PGC-1α-positive cells (arrowheads, Fig. 6E), while little PGC-1α immunoreactivity was detectable on cells with only cell-surface GAD67 (arrows, Fig. 6E). At high magnification it was evident that PGC-1α localized mainly to the nucleus of GAD67-positive neurons (arrowhead, Fig. 6F) with faint staining in the cytoplasm. No PGC-1α was detectable in cellular processes (arrows, Fig. 6F).

In the pyramidal cell layer of the hippocampus at P14, PGC-1α immunoreactivity was concentrated in GAD67-positive neurons (Fig. 6G); faint PGC-1α immunoreactivity was present in GAD67-negative cells. At all postnatal ages studied, PGC-1α immunoreactivity was also localized to GAD67-positive cells throughout the striatum (Fig. 6H), with GAD67-negative cells showing no positivity for PGC-1α. In other areas, including the globus pallidus, reticular nucleus of the thalamus, olfactory bulb, superior and inferior colliculus, and hypothalamus (not shown), PGC-1α also colocalized with GAD67.

In the developing and mature cerebellum, PGC-1α immunoreactivity was localized to several cell types, including Purkinje cells and molecular layer (ML) interneurons (Fig. 7). At P14, PGC-1α was most concentrated in the cell bodies and apical processes of Purkinje cells (arrowheads, Fig. 7A). Cells were still present in the EGL; these were not immunoreactive for PGC-1α (Fig. 7A1). Molecular layer interneurons near the Purkinje cell layer (PL; arrows; Fig. 7A2) were also reactive for PGC-1α. At this stage GAD67 was detectable in Purkinje cell bodies and processes and in some ML interneurons. At P21, the EGL was no longer present, interneurons were more dispersed throughout the ML, and PGC-1α immunoreactivity was concentrated in Purkinje cells (arrowhead; Fig. 7B) and ML interneurons (arrows; Fig. 7B). At this age, GAD67 immunoreactivity was visible throughout the ML and colocalization of PGC-1α and GAD67 was evident (Fig. 7B4). Regarding the expression of PGC-1α in the internal gran-

Fig. 3. The distribution of PGC-1α immunoreactivity parallels that of the neuronal marker NeuN during late embryonic development and localizes to specific cell populations during postnatal cortical development. To investigate the neuroanatomical and cell-specific expression of PGC-1α, the PGC-1α-specific antibody (used for Western blotting; see Fig. 1) was used to detect PGC-1α in brain sections from rats of different developmental ages. **A–F:** Low-magnification images of coronal sections of the E15 rat brain demonstrate that PGC-1α (A) is most concentrated in regions of NeuN and MAP2 immunoreactivity (B,C, respectively; the forming cortical plate), but diffuse in the tubulin-positive intermediate zone (D). At higher magnification it is evident that the immunoreactivity for PGC-1α (E) is concentrated in the cortical plate (CP), similar to NeuN (F), but faint in the cortical neuroepithelium (NE). **G–J:** Immunostaining for PGC-1α and NeuN in sagittal sections of E18 brain reveal that the cortical plate is thicker and remains immunoreactive for PGC-1α (G,I) and NeuN (H,J). **K,L:** In the P3 cortex (sagittal plane), most PGC-1α immunostaining (K) is faint and diffuse, except for a band of cells that shows intense staining (arrowheads). The diffuse staining is in the vicinity of many NeuN-labeled neurons (L). **M,N:** In the P14 cortex, more intensely labeled cells (arrowheads) are noted throughout all cortical layers. **O–Q:** In the adult cortex (sagittal plane), PGC-1α immunoreactivity is mainly cellular, and PGC-1α-labeled cells (O) are less abundant than NeuN-labeled cells (P). Neuronal packing density (higher in Layers IV and VI) and immunoreactivity for glutamic acid decarboxylase 67 (GAD67; Q) allows for identification of cortical layers. In Layers II/III (**R**), a higher proportion of cells show intense immunoreactivity for PGC-1α (arrowheads), than in Layer IV (**S**). In all layers, PGC-1α-immunoreactive cell bodies were small in comparison to faintly stained neurons (arrows). Specificity of staining was confirmed by processing serial sections with rabbit IgG in place of the primary antibody; little immunoreactivity was seen in sections incubated with rabbit IgG (**T**). CP, cortical plate; NE, cortical neuroepithelium; SP, cortical subplate. Scale bars = 300 μm in A–D; E, 100 μm in F,I,J; 200 μm in G,H; 150 μm in K–N; 75 μm in O–Q; 50 μm in R–T.

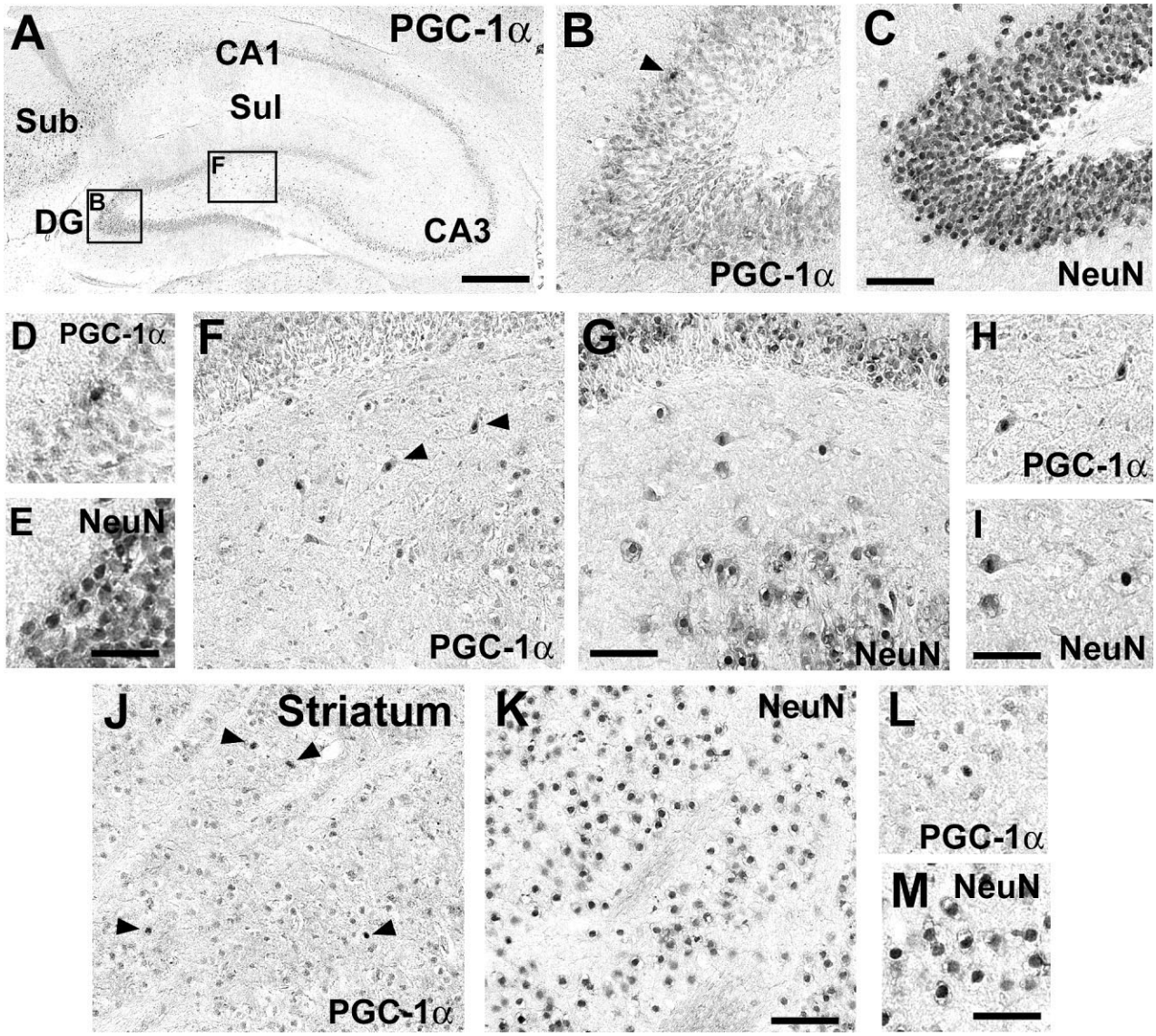

Fig. 4. PGC-1α immunoreactivity is concentrated in specific neurons in the adult hippocampus and striatum. Sagittal sections of adult rat hippocampus and striatum indicate that PGC-1α is most intense in a small number of cells and faint in the majority of other neurons. **A:** At low magnification, faint staining is visible throughout the subiculum (Sub), pyramidal cell layer (CA1 and CA3), and dentate gyrus (DG) of the adult hippocampus. Areas pictured at higher magnification are boxed and lettered accordingly. **B–E:** In the dentate gyrus, faint PGC-1α immunoreactivity (B,D) is observed in most cells in the same location as NeuN-positive neurons (C,E), but one cell shows intense staining (arrowhead, B,D). **F–I:** In the middle of the dentate gyrus, large cells (arrowheads) have a pattern of PGC-1α immunoreactivity (F,H) similar to that for NeuN (G,I), suggesting that PGC-1α is localized to the nucleus of these cells. **J–M:** PGC-1α immunoreactivity is detectable in scattered cells in the striatum as well (J,L); only few cells in the area of NeuN-labeled cells (K,M) show intense immunoreactivity (arrowheads, J; pictured in L). Sub, subiculum; CA1, CA3, cornu ammonis, regions 1 and 3; Sul, hippocampal sulcus; DG, dentate gyrus. Scale bars = 500 μm in A; 100 μm in B,C,F,G,J,K; 40 μm in D,E,H,I,L,M.

ule cell layer (IGL), immunoreactivity was detectable in the IGL in thick sections with light microscopy (see Fig. 5D,E), but in confocal sections it was evident that these cells had the least immunoreactivity of any other cells. Other cells that were GAD67-negative such as cells with the morphology of descending granule cells (black arrowheads, Fig. 7B) were not immunoreactive for PGC-1α.

To confirm that the staining for PGC-1α in the ML was in neurons, we used an antibody for β-tubulin to label neurons and Purkinje cells (Fig. 7C). Most PGC-1α-positive cells in the ML (arrows, Fig. 7C) were immunoreactive for β-tubulin (Fig. 7C3).

Colocalization of PGC-1α with reelin and MEF2

To identify possible functions for PGC-1α during development, we tested whether PGC-1α was present in a specific subpopulation of GABAergic neurons, in particular, neurons that expressed the chemoattractant reelin. This neuronal population is compromised in neurodevelopmen-

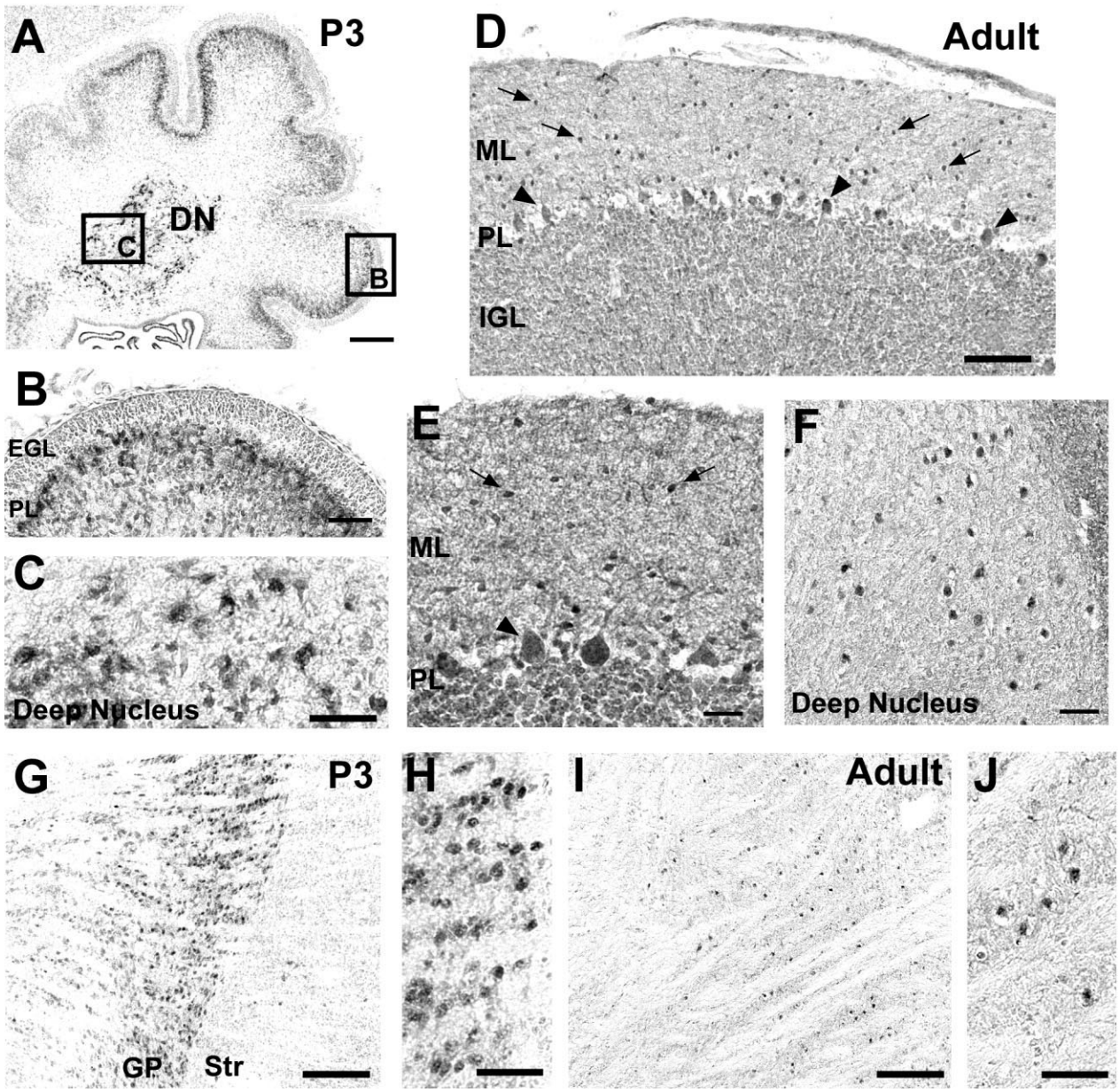

Fig. 5. PGC-1α is expressed abundantly in the cerebellum and globus pallidus in the developing brain. **A–C:** In sagittal sections of the P3 cerebellum, PGC-1α immunoreactivity is visible in the forming Purkinje cell layer (PL; A,B) and the deep nucleus (DN; A,C). Only faint staining is seen in the external granule cell layer (EGL; B). **D–F:** In a sagittal section of the adult cerebellum, PGC-1α immunoreactivity is visible on cell bodies in all cell layers, being the most concentrated in Purkinje cells (arrowheads) and molecular layer interneurons (basket and stellate cells; arrows). Immunoreactivity is also visible on granule cells in the internal granule cell layer (IGL). At this age, neurons of the deep nucleus are also immunoreactive (F). **G,H:** In sagittal sections of P3 forebrain, intense PGC-1α immunoreactivity is found in the globus pallidus (GP). This is in stark contrast to the neighboring striatum (Str), which has only a few scattered PGC-1α-positive cells (see Fig. 4J). **I,J:** PGC-1α-positive cells are also found in the adult globus pallidus, but the density of immunoreactive cells is markedly reduced (G and I are at the same magnification). DN, deep nucleus of the cerebellum; EGL, external granule cell layer; PL, Purkinje cell layer; ML, molecular cell layer; IGL, internal granule cell layer; GP, globus pallidus; Str, striatum. Scale bars = 500 μm in A; 50 μm in B,C,E,F,H,J; 100 μm in D; 200 μm in G,I.

tal disorders such as autism and schizophrenia (Costa et al., 2001; Fatemi, 2005). We found that PGC-1α colocalized with reelin in the cortex and hippocampus from P3 to adulthood (for adult cortex, see Fig. 8A). At all ages reelin was primarily cytoplasmic. Interestingly, both PGC-1α-positive (arrowheads, Fig. 8A) and PGC-1α-negative reelin-positive cells (arrows; Fig. 8A) were identified. Although we were unable to determine whether these reelin-positive PGC-1α-negative neurons were GAD67-negative (because both GAD67 and reelin antibodies were made in mouse), from the literature it is known that ~30% of reelin-positive neurons in the cortex are GAD67-negative,

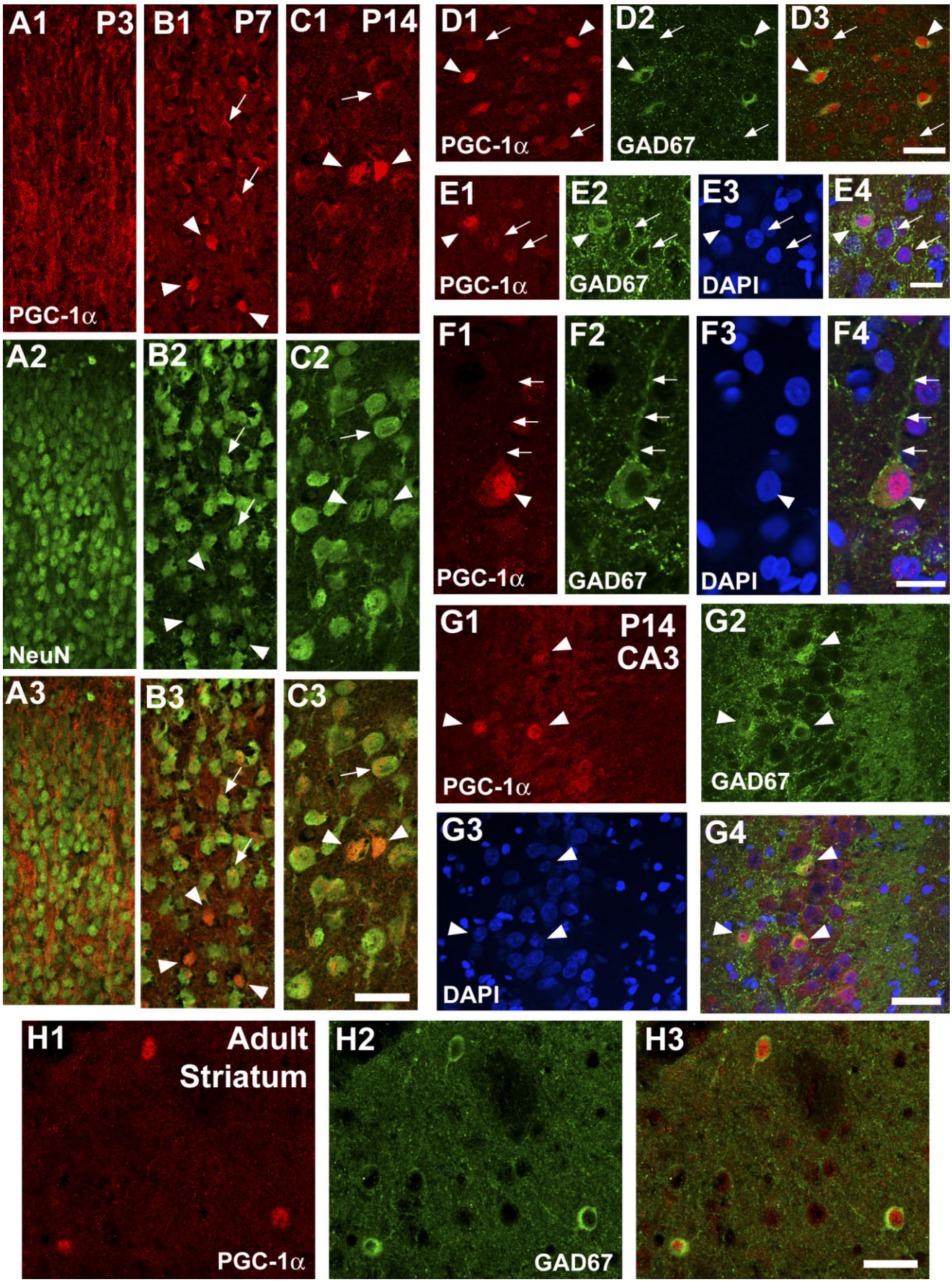
A1
P3
PGC-1α
B1
P7
C1
P14
A2
NeuN
B2
C2
A3
B3
C3
D1
PGC-1α
D2
GAD67
D3
E1
PGC-1α
E2
GAD67
E3
DAPI
E4
F1
PGC-1α
F2
GAD67
F3
DAPI
F4
G1
P14
CA3
PGC-1α
G2
GAD67
G3
DAPI
G4
H1
Adult
Striatum
PGC-1α
H2
GAD67
H3

Figure 6

and ~50% of GABAergic neurons do not express reelin (Pesold et al., 1998). Because all GAD67-positive cells observed in the cortex (P14 and older) expressed PGC-1α, we estimate that at least 50% of PGC-1α-positive cells are reelin-positive in older animals. While PGC-1α colocalized with reelin in the forming cortical plate at E15, PGC-1α did not colocalize with reelin in the distinct band of reelin-positive cells in Layer I during late embryonic and early postnatal development (not shown).

To begin to identify some of the possible factors that can interact with PGC-1α in GABAergic neurons, we determined whether the transcription factor MEF2 was expressed in the same cells as PGC-1α. As expected from previous reports (Lyons et al., 1995), we observed a particular concentration of MEF2 immunoreactivity in the cerebellum (Fig. 8B) in Purkinje cells, ML interneurons, and granule cells. However, we also noted that GAD67-positive neurons in the striatum were intensely immunoreactive for MEF2 (Fig. 8C).

DISCUSSION

Neuronal PGC-1α expression in brain development

Previous studies have shown that mice lacking PGC-1α exhibit neurological abnormalities and vacuolization in various brain regions (Lin et al., 2004; Leone et al., 2005). Interestingly, knockout animals die between birth and 3 weeks of life (50% mortality rate), suggesting that PGC-1α may be developmentally regulated (Lin et al., 2004). In fact, PGC-1α is developmentally regulated in the heart (Lehman and Kelly, 2002), and ectopic expression causes cardiac hypertrophy and mitochondrial proliferation (Russell et al., 2004). Little is known about PGC-1α expression in the brain and whether PGC-1α is expressed during critical periods of brain development, so we used several different methods to evaluate the temporal, regional, and cell-specific expression of PGC-1α in the developing brain. We found that PGC-1α is expressed by neurons throughout the embryonic forebrain and primarily by GABAergic neurons in the early postnatal and adult forebrain and cerebellum. In addition, we determined that PGC-1α mRNA expression peaked at P14 in regions affected in the knockout animals, a time of substantial metabolic changes and synaptic remodeling.

Initially, the Western blot and RT-PCR results seemed discordant; PGC-1α protein expression decreased with age, while mRNA expression was low in embryonic brain and high in early postnatal and mature brain. The Western blot data indicate that PGC-1α constitutes a higher percentage of total protein at earlier ages. This is clearly demonstrated by the immunohistochemistry data showing a decrease in the density of PGC-1α-expressing cells with developmental age (Fig. 5G–J) and the developmental change in location of PGC-1α from widely cytosolic in all neurons to nuclear in GABAergic neurons. The temporal expression of mRNA, however, more closely follows the observation of PGC-1α immunoreactivity in GAD67-positive cells. It is possible that older GABAergic cells have a higher rate of PGC-1α transcription than most early neurons or that younger neurons have a higher rate of protein translation or protein stability. We hypothesize that PGC-1α protein is abundant throughout neuronal cell processes and bodies until P7–P14, at which stage PGC-1α is localized mainly to the nucleus of GABAergic neurons to act as a nuclear transcriptional coactivator. Currently, it is not known whether PGC-1α has any physiological role outside the nucleus. With the limited resolution of the microscopy in samples from embryonic brain, it was impossible to localize extranuclear PGC-1α with any specific organelle.

With immunohistochemistry and immunofluorescence, we failed to detect any PGC-1α in corpus callosum and other white matter tracts, and PGC-1α always colocalized with the neuronal markers NeuN, MAP2, or tubulin. While these results suggest that neurons are the primary source of PGC-1α in the postnatal brain, it is possible that glia express PGC-1α to a lower extent, not detectable by immunohistochemistry and immunofluorescence. Preliminary results from our laboratory suggest that Schwann cells in culture can express PGC-1α when differentiated using adenyl cyclase activators (unpubl. obs., R.M.C.); further experiments are needed to determine whether glia express PGC-1α during differentiation in vivo.

PGC-1α, metabolism, and synaptic plasticity

The critical finding in this study is the specific localization of PGC-1α to the nucleus in GABAergic neurons during the first 3 weeks of life. During this particular phase of brain development, a variety of critical processes are occurring, including a change in mitochondrial dynamics and the initiation of synaptogenesis. Specifically, between P10 and P13 in the rat cortex there is a burst in mitochondrial protein synthesis (Polosa and Attardi, 1991) that corresponds with a sharp increase in cytochrome c oxidase activity, and cytochrome c oxidase IV expression (Cannino et al., 2004). Concurrently, there is a rapid increase in the number of synapses and synaptic vesicles (Jones and Cullen, 1979; Blue and Parnavelas, 1983), oxidative me-

Fig. 6. PGC-1α immunoreactivity colocalizes with the neuronal marker NeuN and glutamic acid decarboxylase (GAD67) in various brain regions throughout development. Postnatal brain tissue was sectioned in the sagittal plane and processed for immunofluorescence and three-color confocal microscopy, using antibodies for PGC-1α (red), NeuN (as a neuronal marker; green), or GAD67 (to identify GABAergic neurons; green). A DAPI counterstain was used to visualize cell nuclei (blue). **A–C:** Immunostained sections through the sensory-motor cortex of P3 (A), P7 (B), and P14 (C) brain reveal that PGC-1α immunoreactivity (A1,B1,C1) is diffuse throughout the cortex at P3 but concentrated in cell bodies at P7 and P14 (arrowheads). When the PGC-1α and NeuN images are overlaid (A3,B3,C3), it is evident that the cellular PGC-1α signal colocalizes with NeuN (arrowheads). At P7 and P14, faint immunoreactivity is visible in other NeuN-positive cells as well (arrows). **D:** At P14 in the cortex, PGC-1α (D1) is concentrated in cells that show intracellular GAD67 immunoreactivity (arrowheads; D2,D3); GAD67-reactive processes are visible throughout the cortex. Faint immunoreactivity is observed in GAD67-neagtive cells (arrows). **E:** In the adult cortex, PGC-1α (E1) is concentrated in GAD67-positive neurons (arrowhead, E2) and faint in neurons that lack cytosolic GAD67 (arrows, E2,E4). In GAD67-positive neurons, PGC-1α colocalizes with DAPI (E3,E4), indicating its presence in the nucleus. **F:** A high-power image of a cortical interneuron demonstrates that PGC-1α (F1) is concentrated mostly in the DAPI-positive nucleus (F3) of GAD67-positive neurons (F2,F4; arrowhead), but that there is also faint immunoreactivity in the cytoplasm. Little PGC-1α is found in neuronal processes in the adult (arrows). **G:** In the hippocampus at P14, PGC-1α (G1) is localized to GAD67-positive neurons (arrowheads, G2) in the pyramidal cell layer (G3). **H:** In the adult striatum, PGC-1α (H1) is concentrated in GAD67-positive cells (H2,H3). No PGC-1α is detectable in GAD67-negative cells. Scale bars = 50 μm in A–D; 20 μm in E,F; 40 μm in G,H.

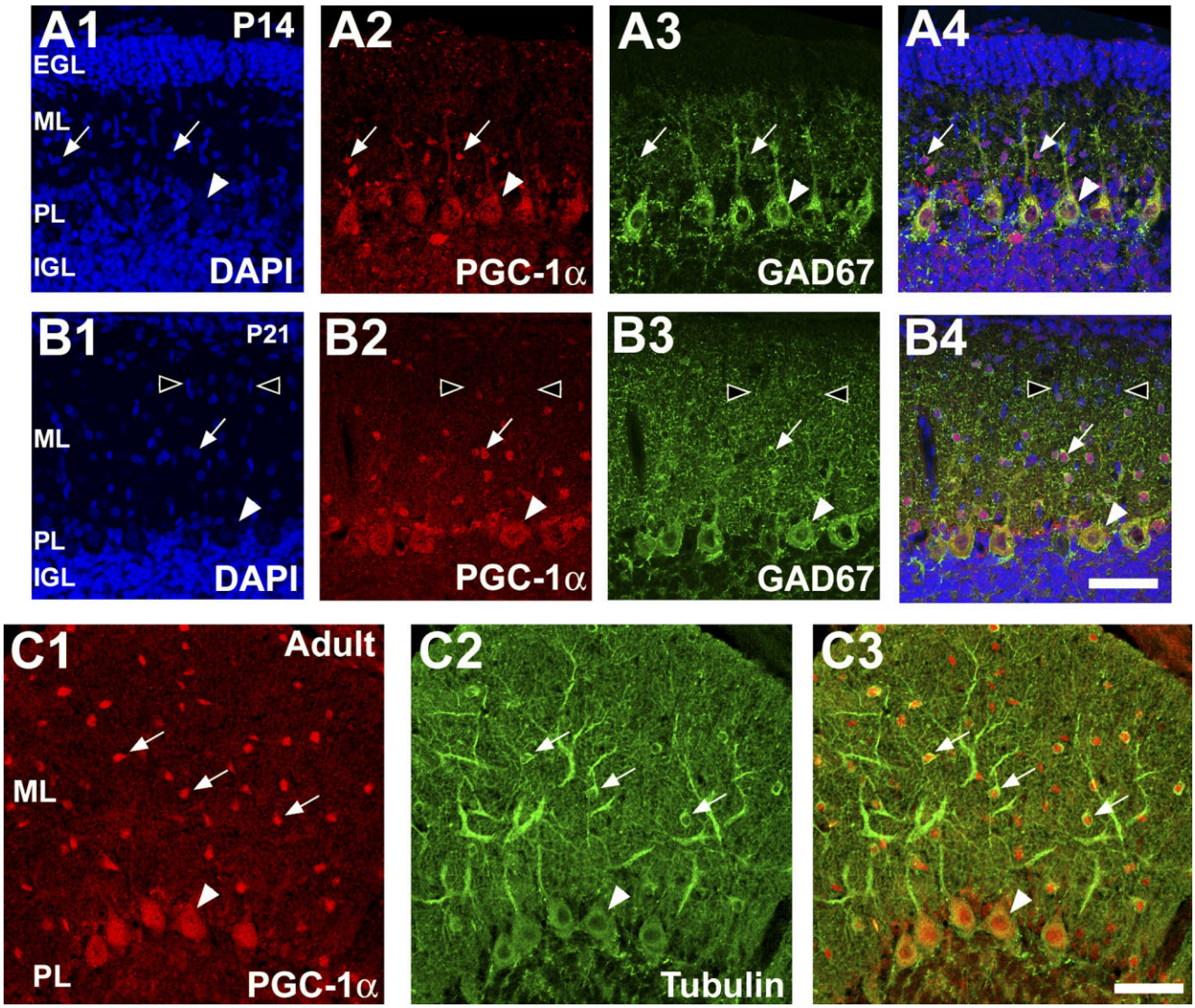

Fig. 7. PGC-1α is expressed in multiple neuronal populations in the developing cerebellum. **A,B:** At all ages tested, PGC-1α immunoreactivity was found in neurons of the cerebellum. Staining with DAPI reveals the cellular layers of the cerebellum at P14 (A1) and P21 (B1). No PGC-1α staining (A2) is visible in the external granule cell layer (EGL) at P14. Instead, PGC-1α is concentrated in GAD67-positive Purkinje cells (A3,A4, arrowheads) and some cell bodies in the lower molecular layer (ML; arrows, A3,A4). PGC-1α staining is faint in the internal granule cell layer (IGL). At P21, no cells remain in the EGL, and no PGC-1α immunoreactivity is detectable on spindle-shaped cells migrating through the ML (black arrows; B1,B2). PGC-1α and GAD67-immunoreactive cells are scattered in the ML (arrow, B2–B4). Purkinje cells express PGC-1α at this age as well (arrowhead, B3,B4). **C:** In the adult cerebellum, PGC-1α (C1) remains concentrated in β-tubulin-positive Purkinje cells (arrowheads, C2) and cells scattered throughout the ML (arrows). Cells with intense PGC-1α immunoreactivity also show β-tubulin reactivity. EGL, external granule cell layer; ML, molecular cell layer; PL, Purkinje cell layer; IGL, internal granule cell layer. Scale bars = 100 μm.

tabolism, and mitochondrial number (Milstein et al., 1968). Of note, these metabolic characteristics are similar to those reported for the brainstem at earlier ages (P3; Liu and Wong-Riley, 2003); the differences in critical metabolic periods in the cortex and brainstem are likely reflective of the caudal-to-rostral development of this system. In fact, PGC-1α immunoreactivity appeared in subcortical structures earlier in development than in cortical structures.

Dendritic mitochondrial dynamics are very important in synaptic plasticity. Increasing mitochondrial activity and/or content has recently been shown to increase synapse density (Li et al., 2004), and mitochondrial proteins are highly expressed at times of plasticity in the developing visual cortex (Yang et al., 2001). Through interactions with the transcription factors NRF-1 and GABP, PGC-1α can upregulate respiratory proteins including cytochrome c oxidase, cytochrome c, and ATPβ synthase (Scarpulla, 2002). The developmental upregulation of PGC-1α could play a role in the increase in mitochondrial activity and number during this time as well as regulating metabolic responses to neuronal activity. Notably, neuronal activity

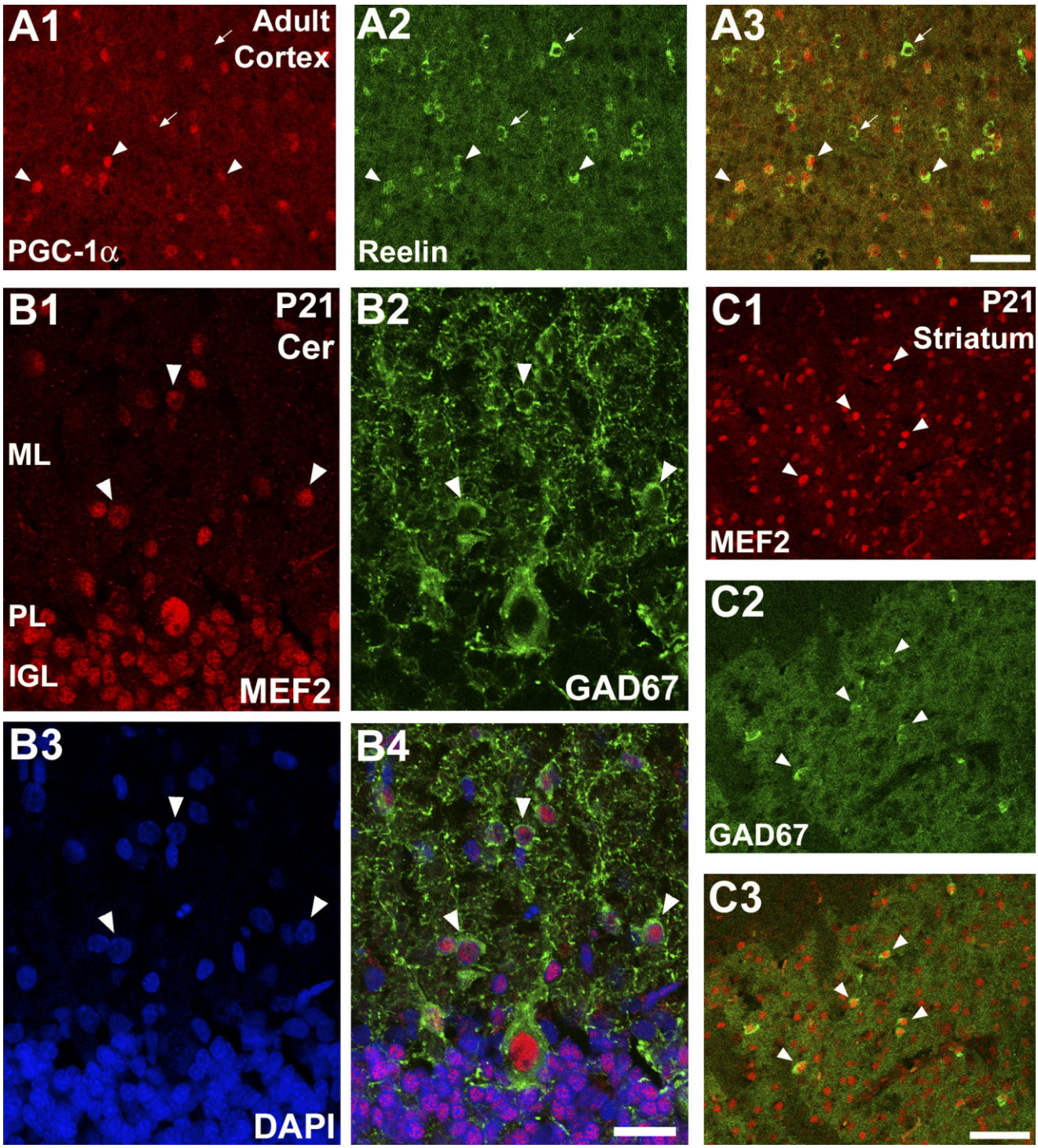

Fig. 8. The chemoattractant reelin and the PGC-1α-binding transcription factor MEF2 are localized to PGC-1α-expressing neurons. Sagittal sections from adult cortex (**A**) and P21 cerebellum (**B**) and striatum (**C**) were processed for immunofluorescence and confocal microscopy with antibodies for PGC-1α, reelin, GAD67, and MEF2. A: In the adult cortex, PGC-1α immunoreactivity (A1) colocalizes with reelin in some cells (arrowheads), but not others (arrows). B,C: Immunoreactivity for the transcription factor MEF2 is found in the same GAD67-positive populations in development as PGC-1α. In the P21 cerebellum (B), a time at which PGC-1α is concentrated in Purkinje cells and molecular layer (ML) interneurons (see Fig. 7), MEF2 is concentrated in GAD67-positive Purkinje cells (large cell body in Purkinje cell layer, PL) and interneurons in the ML (arrowheads), and GAD67-negative granule cells in the internal granule cell layer (IGL). In the P21 striatum, PGC-1α immunoreactivity (C1,C3; red) is found in many neurons, but is most intense in GAD67-positive (green) cells (arrowheads; C2,C3). Scale bars = 100 μm in A,C; 25 μm in B.

causes the translocation of GABP subunits to the nucleus (Yang et al., 2004; Wong-Riley et al., 2005), and putative GABP-binding sites have been identified on all 10 cytochrome c oxidase promoters in vitro (Ongwijitwat and Wong-Riley, 2005).

PGC-1α could also regulate metabolism and cellular energy homeostasis in GABAergic neurons by influencing glucose transport. Glucose transporter GLUT4 is preferentially expressed in parvalbumin-containing GABAergic neurons (Apelt et al., 1999), and PGC-1α overexpression can increase GLUT4 expression in muscle by interacting with MEF-2C (Michael et al., 2001). This is in line with PGC-1α's role as a regulator of glucose homeostasis in other tissues (Rodgers et al., 2005; Wende et al., 2005). Interestingly, GAD67 has also been shown to be glucose-responsive in islet-β cells of the pancreas and C6 glioma cells (Pedersen et al., 2001), and dexamethasone, an agent that stimulates the expression of PGC-1α in liver cells, can increase GAD67 expression in pancreatic β cells (Kim et al., 2002).

PGC-1α and GABA in development

The developmental change in PGC-1α localization from most neurons to mainly GAD67-positive neurons is intriguing. Concentration of immunoreactivity for PGC-1α in cell nuclei occurred around the time that GAD67 first became visible with immunohistochemistry and immunofluorescence. Interestingly, other authors have described a "precocious" band of GAD67 immunoreactivity that appears in Layer V of the developing rat cortex between P3 and P9 (Kiser et al., 1998). This pattern was observed for PGC-1α at P3 (Fig. 3) and P7 (not shown). At present, it is not known whether PGC-1α can directly influence GAD67 expression or metabolism in GABAergic neurons. Preliminary analyses of gene expression in PGC-1α knockout animals have revealed a reduction in GAD67 mRNA expression in whole brain homogenates (unpubl. obs., R.M.C., and J. Lin, University of Michigan). It is also possible that PGC-1α may influence GAD65 expression; although we did not investigate the developmental regulation of GAD65, it has been reported that GAD65 expression in the striatum (Greif et al., 1992), cortex (Kiser et al., 1998), and cerebellum (Greif et al., 1991) is delayed with respect to GAD67. In fact, the appearance of GAD65 coincides with the peak we observed in PGC-1α mRNA expression. As abnormalities in reelin and GAD65/67-positive cells have been linked to autism and schizophrenia (Keverne, 1999; Fatemi, 2005), it would be interesting to investigate whether disruptions in PGC-1α expression contribute to the progression of these disorders.

In the context of this report, the key issue relates to the potential function for PGC-1α in GABAergic neurons during maturation of the rat brain. A critical step in the maturation of GABAergic circuitry occurs during the first 3 postnatal weeks, when the postsynaptic response to GABA changes from excitatory to inhibitory. This change is proposed to be due to the delayed expression of the potassium-chloride transporter KCC2 (Rivera et al., 1999), which when expressed, decreases the intracellular chloride concentration to favor GABA receptor-mediated chloride influx and hyperpolarization. There is a marked increase between P0 and P15 in KCC2 expression in the rat hippocampus and cortex (Herlenius and Lagercrantz, 2004), with high expression levels of KCC2 corresponding to a hyperpolarizing GABA response (Rivera et al., 1999). Interestingly, the temporal profile of KCC2 expression is very similar to that for PGC-1α. At present, it is not clear how PGC-1α expression in presynaptic GABAergic neurons could influence the postsynaptic response to GABA and the expression of KCC2. It would be interesting to speculate that a metabolic boost in GABAergic neurons influences neurotransmitter release and the strengthening of synaptic contacts; in this vein, others have reported that the switch is promoted by activation of GABA receptors, suggesting that the switch could be influenced by presynaptic GABA release in vivo (Ganguly et al., 2001).

These findings are of particular importance with regard to the observed behavioral and neuroanatomical phenotype of the PGC-1α knockout animals. In one knockout model (Lin et al., 2004), mice lacking PGC-1α are hyperactive, showing a 40% increase in the frequency of spontaneous movements. Reduced metabolism in GABAergic neurons due to PGC-1α insufficiency could have a dramatic influence on neurotransmission and neuronal survival, causing postsynaptic overexcitation or excitotoxicity. In fact, PGC-1α knockout animals also exhibit spongiform-like vacuolizations, most often in the dorsolateral striatum (Lin et al., 2004) and in the vicinity of pyramidal neurons in Layer V (Leone et al., 2005). PGC-1α itself may be neuroprotective in GABAergic neurons; PGC-1α can upregulate the expression of antioxidant enzymes (St-Pierre et al., 2003) as well as uncoupling proteins, which have been shown to protect neurons from oxidative stress (Andrews et al., 2005). Along these lines, we found that in the striatum and cerebellum, PGC-1α is expressed in the same cells as MEF2, a transcription factor that plays a role in activity-dependent regulation of neuronal survival (Mao et al., 1999; Okamoto et al., 2002; Deisseroth et al., 2003).

CONCLUSIONS

These findings implicate PGC-1α as a regulator of neuronal function and GABAergic signaling in rat brain development. To determine the functions of PGC-1α more definitively, one must further characterize the transcription factors that are coactivated by PGC-1α in vivo. From what is known about its roles in nonneuronal cells and its distribution described here, PGC-1α is a prime candidate for the transcriptional regulation of metabolism and synaptic plasticity in early postnatal brain development and may be a good target for the treatment of neurodevelopmental and neurodegenerative disorders.

ACKNOWLEDGMENTS

We thank Greg I. Lee for technical assistance with tissue sectioning, Edward J. Brace for advice regarding the citrate buffer technique, Tatsuya Inoue for assistance with RT-PCR, David J. Fink for use of RT-PCR lab equipment and facilities, and Teresa C. Leone for comments on the article. Fluorescence microscopy was performed at the Morphology and Image Analysis Core of the Michigan Diabetes Research and Training Center.

LITERATURE CITED

Al-Bader MD, Al-Sarraf HA. 2005. Housekeeping gene expression during fetal brain development in the rat—validation by semi-quantitative RT-PCR. Brain Res Dev Brain Res 156:38–45.

Allen MP, Xu M, Zeng C, Tobet SA, Wierman ME. 2000. Myocyte enhancer factors-2B and -2C are required for adhesion related kinase repression of neuronal gonadotropin releasing hormone gene expression. J Biol Chem 275:39662–39670.

Amir RE, Van den Veyver IB, Wan M, Tran CQ, Francke U, Zoghbi HY. 1999. Rett syndrome is caused by mutations in X-linked MECP2, encoding methyl-CpG-binding protein 2. Nat Genet 23:185–188.

Andrews ZB, Diano S, Horvath TL. 2005. Mitochondrial uncoupling proteins in the CNS: in support of function and survival. Nat Rev Neurosci 6:829–840.

Apelt J, Mehlhorn G, Schliebs R. 1999. Insulin-sensitive GLUT4 glucose transporters are colocalized with GLUT3-expressing cells and demonstrate a chemically distinct neuron-specific localization in rat brain. J Neurosci Res 57:693–705.

Baar K, Wende AR, Jones TE, Marison M, Nolte LA, Chen M, Kelly DP, Holloszy JO. 2002. Adaptations of skeletal muscle to exercise: rapid increase in the transcriptional coactivator PGC-1. FASEB J 16:1879–1886.

Blue ME, Parnavelas JG. 1983. The formation and maturation of synapses in the visual cortex of the rat. II. Quantitative analysis. J Neurocytol 12:697–712.

Bramlett KS, Burris TP. 2002. Effects of selective estrogen receptor modulators (SERMs) on coactivator nuclear receptor (NR) box binding to estrogen receptors. Mol Genet Metab 76:225–233.

Cannino G, Di Liegro CM, Di Liegro I, Rinaldi AM. 2004. Analysis of cytochrome C oxidase subunits III and IV expression in developing rat brain. Neuroscience 128:91–98.

Costa E, Davis J, Grayson DR, Guidotti A, Pappas GD, Pesold C. 2001. Dendritic spine hypoplasticity and downregulation of reelin and GABAergic tone in schizophrenia vulnerability. Neurobiol Dis 8:723–742.

Czubryt MP, McAnally J, Fishman GI, Olson EN. 2003. Regulation of peroxisome proliferator-activated receptor gamma coactivator 1 alpha (PGC-1 alpha) and mitochondrial function by MEF2 and HDAC5. Proc Natl Acad Sci U S A 100:1711–1716.

Deisseroth K, Mermelstein PG, Xia H, Tsien RW. 2003. Signaling from synapse to nucleus: the logic behind the mechanisms. Curr Opin Neurobiol 13:354–365.

Fatemi SH. 2005. Reelin glycoprotein: structure, biology and roles in health and disease. Mol Psychiatry 10:251–257.

Ganguly K, Schinder AF, Wong ST, Poo M. 2001. GABA itself promotes the developmental switch of neuronal GABAergic responses from excitation to inhibition. Cell 105:521–532.

Greif KF, Erlander MG, Tillakaratne NJ, Tobin AJ. 1991. Postnatal expression of glutamate decarboxylases in developing rat cerebellum. Neurochem Res 16:235–242.

Greif KF, Tillakaratne NJ, Erlander MG, Feldblum S, Tobin AJ. 1992. Transient increase in expression of a glutamate decarboxylase (GAD) mRNA during the postnatal development of the rat striatum. Dev Biol 153:158–164.

Herlenius E, Lagercrantz H. 2004. Development of neurotransmitter systems during critical periods. Exp Neurol 190:S8–21.

Herzig S, Long F, Jhala US, Hedrick S, Quinn R, Bauer A, Rudolph D, Schutz G, Yoon C, Puigserver P, Spiegelman B, Montminy M. 2001. CREB regulates hepatic gluconeogenesis through the coactivator PGC-1. Nature 413:179–183.

Hong EJ, West AE, Greenberg ME. 2005. Transcriptional control of cognitive development. Curr Opin Neurobiol 15:21–28.

Jones DG, Cullen AM. 1979. A quantitative investigation of some presynaptic terminal parameters during synaptogenesis. Exp Neurol 64:245–259.

Kaufman DL, Houser CR, Tobin AJ. 1991. Two forms of the gamma-aminobutyric acid synthetic enzyme glutamate decarboxylase have distinct intraneuronal distributions and cofactor interactions. J Neurochem 56:720–723.

Keverne EB. 1999. GABA-ergic neurons and the neurobiology of schizophrenia and other psychoses. Brain Res Bull 48:467–473.

Kim KS, Kang Y, Choi SE, Kim JH, Kim HM, Sun B, Jun HS, Yoon JW. 2002. Modulation of glucocorticoid-induced GAD expression in pancreatic beta-cells by transcriptional activation of the GAD67 promoter and its possible effect on the development of diabetes. Diabetes 51:2764–2772.

Kiser PJ, Cooper NG, Mower GD. 1998. Expression of two forms of glutamic acid decarboxylase (GAD67 and GAD65) during postnatal development of rat somatosensory barrel cortex. J Comp Neurol 402:62–74.

Knutti D, Kralli A. 2001. PGC-1, a versatile coactivator. Trends Endocrinol Metab 12:360–365.

Kressler D, Schreiber SN, Knutti D, Kralli A. 2002. The PGC-1-related protein PERC is a selective coactivator of estrogen receptor alpha. J Biol Chem 277:13918–13925.

Lehman JJ, Kelly DP. 2002. Transcriptional activation of energy metabolic switches in the developing and hypertrophied heart. Clin Exp Pharmacol Physiol 29:339–345.

Lehman JJ, Barger PM, Kovacs A, Saffitz JE, Medeiros DM, Kelly DP. 2000. Peroxisome proliferator-activated receptor gamma coactivator-1 promotes cardiac mitochondrial biogenesis. J Clin Invest 106:847–856.

Leone TC, Lehman JJ, Finck BN, Schaeffer PJ, Wende AR, Boudina S, Courtois M, Wozniak DF, Sambandam N, Bernal-Mizrachi C, Chen Z, Holloszy JO, Medeiros DM, Schmidt RE, Saffitz JE, Abel ED, Semenkovich CF, Kelly DP. 2005. PGC-1alpha deficiency causes multi-system energy metabolic derangements: muscle dysfunction, abnormal weight control and hepatic steatosis. PLoS Biol 3:e101.

Li Z, Okamoto K, Hayashi Y, Sheng M. 2004. The importance of dendritic mitochondria in the morphogenesis and plasticity of spines and synapses. Cell 119:873–887.

Liang HL, Wong-Riley MT. 2006. Activity-dependent regulation of nuclear respiratory factor-1, nuclear respiratory factor-2, and peroxisome proliferator-activated receptor gamma coactivator-1 in neurons. Neuroreport 17:401–405.

Lin J, Tarr PT, Yang R, Rhee J, Puigserver P, Newgard CB, Spiegelman BM. 2003. PGC-1beta in the regulation of hepatic glucose and energy metabolism. J Biol Chem 278:30843–30848.

Lin J, Wu PH, Tarr PT, Lindenberg KS, St-Pierre J, Zhang CY, Mootha VK, Jager S, Vianna CR, Reznick RM, Cui L, Manieri M, Donovan MX, Wu Z, Cooper MP, Fan MC, Rohas LM, Zavacki AM, Cinti S, Shulman GI, Lowell BB, Krainc D, Spiegelman BM. 2004. Defects in adaptive energy metabolism with CNS-linked hyperactivity in PGC-1alpha null mice. Cell 119:121–135.

Liu Q, Wong-Riley MT. 2003. Postnatal changes in cytochrome oxidase expressions in brain stem nuclei of rats: implications for sensitive periods. J Appl Physiol 95:2285–2291.

Lyons GE, Micales BK, Schwarz J, Martin JF, Olson EN. 1995. Expression of mef2 genes in the mouse central nervous system suggests a role in neuronal maturation. J Neurosci 15:5727–5738.

Mao Z, Bonni A, Xia F, Nadal-Vicens M, Greenberg ME. 1999. Neuronal activity-dependent cell survival mediated by transcription factor MEF2. Science 286:785–790.

Michael LF, Wu Z, Cheatham RB, Puigserver P, Adelmant G, Lehman JJ, Kelly DP, Spiegelman BM. 2001. Restoration of insulin-sensitive glucose transporter (GLUT4) gene expression in muscle cells by the transcriptional coactivator PGC-1. Proc Natl Acad Sci U S A 98:3820–3825.

Milstein JM, White JG, Swaiman KF. 1968. Oxidative phosphorylation in mitochondria of developing rat brain. J Neurochem 15:411–415.

Nisoli E, Clementi E, Paolucci C, Cozzi V, Tonello C, Sciorati C, Bracale R, Valerio A, Francolini M, Moncada S, Carruba MO. 2003. Mitochondrial biogenesis in mammals: the role of endogenous nitric oxide. Science 299:896–899.

Okamoto S, Li Z, Ju C, Scholzke MN, Mathews E, Cui J, Salvesen GS, Bossy-Wetzel E, Lipton SA. 2002. Dominant-interfering forms of MEF2 generated by caspase cleavage contribute to NMDA-induced neuronal apoptosis. Proc Natl Acad Sci U S A 99:3974–3979.

Ongwijitwat S, Wong-Riley MT. 2005. Is nuclear respiratory factor 2 a master transcriptional coordinator for all ten nuclear-encoded cytochrome c oxidase subunits in neurons? Gene 360:65–77.

Pedersen AA, Videbaek N, Skak K, Petersen HV, Michelsen BK. 2001. Characterization of the rat GAD67 gene promoter reveals elements important for basal transcription and glucose responsiveness. DNA Seq 11:485–499.

Pesold C, Impagnatiello F, Pisu MG, Uzunov DP, Costa E, Guidotti A, Caruncho HJ. 1998. Reelin is preferentially expressed in neurons synthesizing gamma-aminobutyric acid in cortex and hippocampus of adult rats. Proc Natl Acad Sci U S A 95:3221–3226.

Petrij F, Giles RH, Dauwerse HG, Saris JJ, Hennekam RC, Masuno M, Tommerup N, van Ommen GJ, Goodman RH, Peters DJ, et al. 1995. Rubinstein-Taybi syndrome caused by mutations in the transcriptional co-activator CBP. Nature 376:348–351.

Polosa PL, Attardi G. 1991. Distinctive pattern and translational control of mitochondrial protein synthesis in rat brain synaptic endings. J Biol Chem 266:10011–10017.

Puigserver P, Wu Z, Park CW, Graves R, Wright M, Spiegelman BM. 1998.

A cold-inducible coactivator of nuclear receptors linked to adaptive thermogenesis. Cell 92:829–839.

Rivera C, Voipio J, Payne JA, Ruusuvuori E, Lahtinen H, Lamsa K, Pirvola U, Saarma M, Kaila K. 1999. The K+/Cl- co-transporter KCC2 renders GABA hyperpolarizing during neuronal maturation. Nature 397:251–255.

Rodgers JT, Lerin C, Haas W, Gygi SP, Spiegelman BM, Puigserver P. 2005. Nutrient control of glucose homeostasis through a complex of PGC-1alpha and SIRT1. Nature 434:113–118.

Russell LK, Mansfield CM, Lehman JJ, Kovacs A, Courtois M, Saffitz JE, Medeiros DM, Valencik ML, McDonald JA, Kelly DP. 2004. Cardiac-specific induction of the transcriptional coactivator peroxisome proliferator-activated receptor gamma coactivator-1alpha promotes mitochondrial biogenesis and reversible cardiomyopathy in a developmental stage-dependent manner. Circ Res 94:525–533.

Scarpulla RC. 2002. Nuclear activators and coactivators in mammalian mitochondrial biogenesis. Biochim Biophys Acta 1576:1–14.

Schmittgen TD, Zakrajsek BA. 2000. Effect of experimental treatment on housekeeping gene expression: validation by real-time, quantitative RT-PCR. J Biochem Biophys Methods 46:69–81.

Schreiber SN, Emter R, Hock MB, Knutti D, Cardenas J, Podvinec M, Oakeley EJ, Kralli A. 2004. The estrogen-related receptor alpha (ERRalpha) functions in PPARgamma coactivator 1alpha (PGC-1alpha)-induced mitochondrial biogenesis. Proc Natl Acad Sci U S A 101:6472–6477.

St-Pierre J, Lin J, Krauss S, Tarr PT, Yang R, Newgard CB, Spiegelman BM. 2003. Bioenergetic analysis of peroxisome proliferator-activated receptor gamma coactivators 1alpha and 1beta (PGC-1alpha and PGC-1beta) in muscle cells. J Biol Chem 278:26597–26603.

Tiraby C, Tavernier G, Lefort C, Larrouy D, Bouillaud F, Ricquier D, Langin D. 2003. Acquirement of brown fat cell features by human white adipocytes. J Biol Chem 278:33370–33376.

Tritos NA, Mastaitis JW, Kokkotou EG, Puigserver P, Spiegelman BM, Maratos-Flier E. 2003. Characterization of the peroxisome proliferator activated receptor coactivator 1 alpha (PGC 1alpha) expression in the murine brain. Brain Res 961:255–260.

Villena JA, Vinas O, Mampel T, Iglesias R, Giralt M, Villarroya F. 1998. Regulation of mitochondrial biogenesis in brown adipose tissue: nuclear respiratory factor-2/GA-binding protein is responsible for the transcriptional regulation of the gene for the mitochondrial ATP synthase beta subunit. Biochem J 331:121–127.

Wende AR, Huss JM, Schaeffer PJ, Giguere V, Kelly DP. 2005. PGC-1alpha coactivates PDK4 gene expression via the orphan nuclear receptor ERRalpha: a mechanism for transcriptional control of muscle glucose metabolism. Mol Cell Biol 25:10684–10694.

Wong-Riley MT, Yang SJ, Liang HL, Ning G, Jacobs P. 2005. Quantitative immuno-electron microscopic analysis of nuclear respiratory factor 2 alpha and beta subunits: normal distribution and activity-dependent regulation in mammalian visual cortex. Vis Neurosci 22:1–18.

Yang C, Silver B, Ellis SR, Mower GD. 2001. Bidirectional regulation of mitochondrial gene expression during developmental neuroplasticity of visual cortex. Biochem Biophys Res Commun 287:1070–1074.

Yang SJ, Liang HL, Ning G, Wong-Riley MT. 2004. Ultrastructural study of depolarization-induced translocation of NRF-2 transcription factor in cultured rat visual cortical neurons. Eur J Neurosci 19:1153–1162.

Yoon JC, Puigserver P, Chen G, Donovan J, Wu Z, Rhee J, Adelmant G, Stafford J, Kahn CR, Granner DK, Newgard CB, Spiegelman BM. 2001. Control of hepatic gluconeogenesis through the transcriptional coactivator PGC-1. Nature 413:131–138.

Zhang Y, Ma K, Song S, Elam MB, Cook GA, Park EA. 2004. Peroxisomal proliferator-activated receptor-gamma coactivator-1 alpha (PGC-1 alpha) enhances the thyroid hormone induction of carnitine palmitoyltransferase I (CPT-I alpha). J Biol Chem 279:53963–53971.